

Supplementary Information

Filling the Gaps in the Kirromycin Biosynthesis: Deciphering the Role of Genes Involved in Ethylmalonyl-CoA Supply and Tailoring Reactions

Helene L. Robertsen^{a,1}, Ewa M. Musiol-Kroll^{a,1,2,3}, Ling Ding¹, Kristina J. Laiple²,
Torben Hofeditz⁴, Wolfgang Wohlleben^{2,3}, Sang Yup Lee^{1,5}, Stephanie Grond⁴, and
Tilmann Weber¹

^aEqual contribution

¹Novo Nordisk Foundation Center for Biosustainability, Technical University of
Denmark, Kemitorvet 220, 2800 Kgs. Lyngby, Denmark

²Eberhard-Karls-Universität Tübingen, Interfakultäres Institut für Mikrobiologie und
Infektionsmedizin, Microbiology/Biotechnology, Auf der Morgenstelle 28, 72076
Tübingen, Germany

³German Centre for Infection Research (DZIF), Partner site Tübingen, Auf der
Morgenstelle 28, 72076 Tübingen, Germany

⁴Eberhard-Karls-Universität Tübingen, Institut für Organische Chemie, Auf der
Morgenstelle 18, 72076 Tübingen, Germany

⁵Department of Chemical and Biomolecular Engineering (BK21 Plus Program),
Korea Advanced Institute of Science and Technology (KAIST), 291 Daehak-ro,
Yuseong-gu, Daejeon 305-701, Republic of Korea

Table of Contents

Table S1: Strains and plasmids in this study.....	3
Table S2: Primers used in this study.....	6
Table S3: HPLC-ESI-HRMS data for kirromycin and derivatives.....	9
Table S4: ¹ H NMR spectra and assignments.....	10
Figure S1-I – S1-II: UV-VIS profiles of $\Delta kirHIV$ and $\Delta kirHV$ mutants	14
Figure S2-I – S2-V: MS/MS spectra of kirromycin and derivatives.....	15
Figure S3-I – S3-VI: HPLC-ESI-UV-Vis profiles of the wild type (WT), Δkir mutants, and complemented mutants	18
Figure S4-IA/B – S4-IIA/B: ¹ H NMR and ¹³ C NMR data and assignment for 30-deoxy-kirromycin (3), 5,6-dihydro-kirromycin (4), and 30-hydroxy-5,6-dehydro-1- <i>N</i> -demethyl-16-deoxy-kirrothricin (5)	21
Figure S5-I – S5-III: 2D-NMR of 30-deoxy-kirromycin (3), 5,6-dihydro-kirromycin (4), and 30-hydroxy-5,6-dehydro-1- <i>N</i> -demethyl-16-deoxy-kirrothricin (5)	25
Figure S6-I – S6-II: Verification of Δkir mutants by control PCRs.....	35
Figure S7-I – S7-III: Putative enzymatic reactions catalysed by tailoring enzymes KirHVI, KirOI, and KirOII.....	36
Supplementary references.....	38

Table S1: Strains and plasmids in this study

Source	Description/Genotype	Reference
<i>E. coli</i> strains		
<i>E. coli</i> DH5- α	<i>fhuA2</i> , $\Delta(\text{argF-lacZ})\text{U169}$, <i>phoA</i> , <i>glnV44</i> , $\Phi 80$, $\Delta(\text{lacZ})\text{M15}$, <i>gyrA96</i> , <i>recA1</i> , <i>relA1</i> , <i>endA1</i> , <i>thi-1</i> , <i>hsdR17</i>	New England Biolabs
<i>E. coli</i> ET12567 (pUZ8002)	<i>dam13::Tn9(ChlR)</i> , <i>dcm-6</i> , <i>hsdM</i> , <i>hsdR</i> , <i>recF143</i> , <i>zjj-201::Tn10</i> , <i>galK2</i> , <i>galT22</i> , <i>ara14</i> , <i>lacY1</i> , <i>xyl-5</i> , <i>leuB6</i> , <i>thi-1</i> , <i>tonA31</i> , <i>rpsL136</i> , <i>hisG4</i> , <i>tsx-78</i> , <i>mtII</i> , <i>glnV44</i> . pUZ8002(KanR)	1
<i>Streptomyces</i> strains		
<i>S. collinus</i> Tü 365	Wild type <i>Streptomyces collinus</i> Tü 365	2
ΔkirM	<i>S. collinus</i> Tü 365 deletion mutant in <i>kirM</i>	This study
ΔkirHVI	<i>S. collinus</i> Tü 365 deletion mutant in <i>kirHVI</i>	This study
ΔkirOI	<i>S. collinus</i> gene replacement mutant in which <i>kirOI</i> is replaced by the thiostrepton resistance cassette with the <i>ermE*</i> promoter downstream. ThioR	This study
ΔkirOII	<i>S. collinus</i> gene replacement mutant in which <i>kirOII</i> is replaced by the thiostrepton resistance cassette with the <i>ermE*</i> promoter downstream. ThioR	This study
ΔkirHIV	<i>S. collinus</i> Tü 365 deletion mutant in <i>kirHIV</i>	This study
ΔkirHV	<i>S. collinus</i> Tü 365 deletion mutant in <i>kirHV</i>	This study
ΔkirN	<i>S. collinus</i> Tü 365 deletion mutant in <i>kirN</i>	This study
$\Delta\text{kirOI-pGM1190}$	ΔkirOI complemented with replicative plasmid pGM1190- <i>kirOI</i> . ApraR, ThioR	This study
$\Delta\text{kirM-pRM4}$	ΔkirM complemented with integrative plasmid pRM4- <i>kirM</i> . ApraR	This study
$\Delta\text{kirHVI-pRM4}$	ΔkirHVI complemented with integrative plasmid pRM4- <i>kirHVI</i> . ApraR	This study
$\Delta\text{kirOII-pRM4}$	ΔkirOII complemented with integrative plasmid pRM4- <i>kirOII</i> . ApraR, ThioR	This study
$\Delta\text{kirN-pRM4}_1$	ΔkirN complemented with integrative plasmid pRM4- <i>kirHVI</i> . ApraR	This study
$\Delta\text{kirN-pRM4}_2$	ΔkirN complemented with integrative plasmid pRM4- <i>kirN+HVI</i> . ApraR	This study
Cosmids		
1C24	pOJ436 cosmid vector with a fragment of the genome of kirromycin producer <i>Streptomyces collinus</i> Tü 365	3
2K05	pOJ436 cosmid vector with a fragment of the genome of kirromycin producer <i>Streptomyces collinus</i> Tü 365	3
Plasmids		
pJet1.2/blunt	<i>rep</i> (pMB1), <i>bla</i> (AmpR), <i>eco47IR</i> , PlacUV5, T7 RNA polymerase promoter. Part of the CloneJET™ PCR Cloning Kit used for high efficiency cloning of PCR products	Thermo Fisher Scientific Inc.
pDrive	T7 RNA polymerase promoter, LacZ α , SP6 RNA polymerase promoter, AmpR, KanR, pUC origin, phage f1 origin of replication. For construction of ΔkirOI and ΔkirOII gene inactivation plasmids	Qiagen
pGUSA21	Promoter probe vector, pSETGUS with deleted KpnI fragment containing TipA promoter. <i>gusA</i> , Δint , ΔattB , MCS from pUC21. Used for gene inactivation	4

Source	Description/Genotype	Reference
pGM1190	pGM190 derivative in which the kanamycin resistance cassette is exchanged with the apramycin resistance gene <i>aac3(3)IV</i> . TipA promoter. ApraR, ThioR. Used for complementation of the $\Delta kirOI$ mutant	G. Muth (personal communication)
pRM4	pSET152 <i>ermEp</i> derivative with an artificial RBS, $\Phi C31$ integration vector, <i>ermE*</i> promoter. ApraR. Used for complementation of the <i>kir</i> mutants	5
pA18mob	pK18mob derivative in which <i>aphII</i> is replaced with the apramycin resistance cassette. <i>oriT</i> , <i>lacZa</i> . ApraR. Used for construction of gene replacement mutants of <i>kirOI</i> and <i>kirOII</i> .	3
pSLE61	pUC19 derivative. <i>lacZa</i> , <i>oriI</i> , pSG5 replicon. AmpR, ThioR. For amplification of thiostrepton resistance cassette	6
pCRISPR-Cas9	Derivative of pGM1190 with Cas9 under the control of TipA promoter	7
pCRISPR-Cas9_USER- $\Delta kirM$	USER-compatible destination vector, which is a derivative of pGM1190 with Cas9 under the control of TipA promoter. Cloned with <i>ermE*</i> promoter between sgRNA and 1 kb flanking regions right and left of <i>kirM</i> inserted in the USER cassette. ApraR	7,8
pCRISPR-Cas9_USER- $\Delta kirHIV$	USER-compatible destination vector, which is a derivative of pGM1190 with Cas9 under the control of TipA promoter. Cloned with <i>ermE*</i> promoter between sgRNA and 1 kb flanking regions right and left of <i>kirHIV</i> inserted in the USER cassette. ApraR	7,8
pCRISPR-Cas9_USER- $\Delta kirHV$	USER-compatible destination vector, which is a derivative of pGM1190 with Cas9 under the control of TipA promoter. Cloned with <i>ermE*</i> promoter between sgRNA and 1 kb flanking regions right and left of <i>kirHV</i> inserted in the USER cassette. ApraR	7,8
pCRISPR-Cas9_USER- $\Delta kirN$	USER-compatible destination vector, which is a derivative of pGM1190 with Cas9 under the control of TipA promoter. Cloned with <i>ermE*</i> promoter between sgRNA and 1 kb flanking regions right and left of <i>kirN</i> inserted in the USER cassette. ApraR	7,8
pHR1	pGUSA21 deletion plasmid of <i>kirM</i> cloned with <i>ermE*</i> promoter between 1 kb flanking regions of the gene. 2.1 kb construct cloned from pCRISPR-Cas9_USER- <i>kirM</i> . ApraR	This study
pHR2	pGUSA21 deletion plasmid of <i>kirHVI</i> cloned with <i>ermE*</i> promoter between 1 kb flanking regions of the gene. ApraR	This study
pHR3	pGUSA21 deletion plasmid of <i>kirHIV</i> cloned with <i>ermE*</i> promoter between 1 kb flanking regions of the gene. 2.1 kb construct cloned from pCRISPR-Cas9_USER- <i>kirHIV</i> . ApraR	This study
pHR4	pGUSA21 deletion plasmid of <i>kirHV</i> cloned with <i>ermE*</i> promoter between 1 kb flanking regions of the gene. 2.1 kb construct cloned from pCRISPR-Cas9_USER- <i>kirHV</i> . ApraR	This study
pHR5	pGUSA21 deletion plasmid of <i>kirN</i> cloned with <i>ermE*</i> promoter between 1 kb flanking regions of the gene. 2.1 kb construct cloned from pCRISPR-Cas9_USER- <i>kirN</i> . ApraR	This study
pTL- <i>kirOI</i>	1.2 kb flanking regions left and right of <i>kirOI</i> cloned in pA18mob. ApraR	This study
pTL- <i>kirOI</i> -thio	pTL- <i>kirOI</i> cloned with thiostrepton resistance cassette	This study

Source	Description/Genotype	Reference
	inserted in XbaI site. ApraR, ThioR	
pDW- <i>kirOII</i>	2 kb flanking regions left and right of <i>kirOII</i> cloned in pA18mob. ApraR	This study
pDW- <i>kirOII</i> -thio	pDW- <i>kirOII</i> cloned with thioStreptomycin resistance cassette inserted in the XbaI site. ApraR, ThioR	This study
pJet1.2- <i>kirM</i>	pJet1.2/blunt with <i>kirM</i> cloned in the MCS. AmpR	This study
pJet1.2- <i>kirHVI</i>	pJet1.2/blunt with <i>kirHVI</i> cloned in the MCS. AmpR	This study
pJet1.2- <i>kirOI</i>	pJet1.2/blunt with <i>kirOI</i> cloned in the MCS. AmpR	This study
pJet1.2- <i>kirOII</i>	pJet1.2/blunt with <i>kirOII</i> cloned in the MCS. AmpR	This study
pJet1.2- <i>kirN</i>	pJet1.2/blunt with <i>kirN</i> cloned in the MCS. AmpR	This study
pJet1.2- <i>kirN+HVI</i>	pJet1.2/blunt with <i>kirN+HVI</i> cloned in the MCS. AmpR	This study
pGM1190- <i>kirOI</i>	pGM1190 with <i>kirOI</i> cloned in HindIII + EcoRI site	This study
pRM4- <i>kirM</i>	pRM4 with <i>kirM</i> cloned in NdeI + HindIII site	This study
pRM4- <i>kirHVI</i>	pRM4 with <i>kirHVI</i> cloned in NdeI + HindIII site	This study
pRM4- <i>kirOII</i>	pRM4 with <i>kirOII</i> cloned in NheI + HindIII site	This study
pRM4- <i>kirN</i>	pRM4 with of <i>kirN</i> cloned in NdeI + HindIII site	This study
pRM4- <i>kirN+HVI</i>	pRM4 with <i>kirN+kirHVI</i> cloned in NdeI + HindIII site	This study

Table S2: Primers used in this study

ID	Primer name	Sequence (5' - 3')	PCR program
<i>kirM, kirN, kirHIV, and kirHV</i> inactivation mutants			
KP1	kirM_pGUS_left_FW	CTGCAGACGCGTCGACGTCGAAGC GACGAGGAGCTGGCG	1. 98°C, 0:30 min 2. 98°C, 0:10 min 3. 73°C, 0:30 min 4. 72°C, 1:00 min 5. 72°C, 5:00 min (Steps 2-4 × 34)
KP2	kirM_pGUS_left_RV	ATTACCTGTTATCCCTAGTTAGT ACGCGGGCCCCAGG	
KP3	kirN_pGUS_left_FW	GGAGCTCGAATTCGAAGCTTCTG CAGACGCGTCGACGTCATATGCG ACCCCGACCAGGA	1. 98°C, 0:30 min 2. 98°C, 0:10 min 3. 75°C, 0:30 min 4. 72°C, 1:00 min 5. 72°C, 5:00 min (Steps 2-4 × 34)
KP4	kirN_pGUS_right_RV	GCGGGAAGCAGTGATAAGCATT ACCCTGTTATCCCTAGTTCTAGA ATCTCCGACGACGCGT	
KP5	kirHIV_pGUS_left_FW	GCAGACGCGTCGACGTCACTGCT CAAGTACTTCGACTCGAC	1. 98°C, 0:30 min 2. 98°C, 0:10 min 3. 70°C, 0:30 min 4. 72°C, 1:00 min 5. 72°C, 5:00 min (Steps 2-4 × 34)
KP6	kirHIV_pGUS_right_RV	ATTACCTGTTATCCCTAGTTTGA CCAGCGCCAGTTGTG	
KP7	kirHV_pGUS_left_FW	CTGCAGACGCGTCGACGTCAGCT CAGCTTCGCCGC	1. 98°C, 0:30 min 2. 98°C, 0:10 min 3. 73°C, 0:30 min 4. 72°C, 1:00 min 5. 72°C, 5:00 min (Steps 2-4 × 34)
KP8	kirHV_pGUS_right_RV	ATTACCTGTTATCCCTAGTTGA CGATGTCGGGATCCTCCC	
<i>kirHVI</i> inactivation mutant			
KP9	kirHVI_pGUS_left_FW	GACGCGTCGACGTCACCGGAGTC GTGCTG	1. 98°C, 0:30 min 2. 98°C, 0:10 min 3. 72°C, 0:30 min 4. 72°C, 0:30 min 5. 72°C, 5:00 min (Steps 2-4 × 34)
KP10	kirHVI_pGUS_left_RV	GTCAAGATCGACCGCTTGTTCC CTTCCCTG	
KP11	kirHVI_pGUS_ermE_FW	CTACAGGGAAGGGAAACAAGCG GTCGATCTTGACG	1. 98°C, 0:30 min 2. 98°C, 0:10 min 3. 74°C, 0:10 min 4. 72°C, 1:00 min 5. 72°C, 5:00 min (Steps 2-4 × 34)
KP12	kirHVI_pGUS_ermE_RV	CGACGGGCGGCTCGCCGTCGATC CTACCAA	
KP13	kirHVI_pGUS_right_FW	GGTAGGATCGACGGCGAGCCGC CCGTCG	1. 98°C, 0:30 min 2. 98°C, 0:10 min 3. 75°C, 0:30 min 4. 72°C, 0:30 min 5. 72°C, 5:00 min (Steps 2-4 × 34)
KP14	kirHVI_pGUS_right_RV	ATTACCTGTTATCCCTAGTTGG ACGCGACCAGGCCGC	

ID	Primer name	Sequence (5' - 3')	PCR program
<i>kirOI</i> and <i>kirOII</i> inactivation mutants			
KP15	1ldOxy5	AACTGCAGTCAACATCACCTACG ACC	1. 94°C, 2:00 min 2. 94°C, 1:15 min 3. 60°C, 1:30 min 4. 72°C, 1:30 min 5. 72°C, 5:00 min (Steps 2-4 × 30)
KP16	1ldOxy3	AATCTAGACTCGTCGTAGCCGGT G	
KP17	1rdOxy5	AATCTAGAGTCGGCCAGCAACTG G	
KP18	1rdOxy3	AAGAATTTCGAACACGTCGATGTG CG	
KP19	thio-up	ACTCTAGATCACTGACGAATCGA GGTCGAGGA	
KP20	thio-low	AATCTAGAGGCGAATACTTCATA TGCGGGGAT	
KP21	leftOIIeco5	GAATTCGTGCCAGGAGGTGATCC	1. 94°C, 2:00 min 2. 94°C, 1:15 min 3. 60°C, 1:30 min 4. 72°C, 2:00 min 5. 72°C, 5:00 min (Steps 2-4 × 30)
KP22	leftOIIxba3	TCTAGACTCGACGTCCGTCCAAT C	
KP23	rightOIIxba5	TCTAGAGGCCCGCGCTTCTGAA AG	
KP24	rightOIIhind3	AAGCTTCAGCGCGAACTGCGTCG	
Complementation plasmids			
KP27	kirN_NdeI_FW	AAACATATGCAAGACATCATCGA CGCCG	1. 98°C, 0:30 min 2. 98°C, 0:10 min 3. 60°C, 0:30 min 4. 72°C, * 5. 72°C, 5:00 min (Steps 2-4 × 34)
KP28	kirN_HindIII_RV	AAAAAGCTTTTCATTTGTTTCCCTT CCCTGTAGG	
KP29	kirM_NdeI_FW	AAACATATGAGCCAACCCGATGT GATGACC	
KP30	kirM_HindIII_RV	AAAAAGCTTTCAGACTCGGACGG CGAC	
KP31	kirHVI_NdeI_FW	AAACATATGACCGACGAAGACC TCGTACCG	
KP32	kirHVI_HindIII_RV	AAAAAGCTTTC AACCGGCGCGCT CGG	
KP33	kirOI_HindIII_pGM1190_FW	AAAAAGCTTGTGTCCGAGACCGT TCGTCCCCG	
KP34	kirOI_EcoRI_pGM1190_RV	AAAGAATTCTCACCATGTCACCG GCAGCTCG	
KP35	kirOII_NheI_FW	AAAGCTAGCGTGACCGGAACATT CGATTGGACG	
KP36	kirOII_HindIII_RV	AAAAAGCTTTCACACGAGCTGGA CGGGCAG	
Control PCRs and sequencing			
KP37	kirLEFT_pGUS_seq_FW	GCTCGAATTCGAAGCTTCTGCAG	1. 95°C, 3:00 min 2. 95°C, 0:30 min 3. 61°C, 0:30 min 4. 72°C, 2:15 min 5. 72°C, 5:00 min (Steps 2-4 × 40)
KP38	kirRIGHT_pGUS_seq_RV	GATAAGCATTACCCTGTTATCCC TAG	
KP39	apra-up	AGCTTCTCAACCTTGG	1. 94°C, 2:00 min 2. 94°C, 1:00 min 3. 50°C, 1:00 min 4. 72°C, 1:00 min 5. 72°C, 5:00 min (Steps 2-4 × 30)
KP40	apra-low	TCCGCCAAGGCAAAGC	

ID	Primer name	Sequence (5' - 3')	PCR program
KP41	oxy1	GCAAAGGAGAGCGTTGTGTC	1. 94°C, 2:00 min 2. 94°C, 1:00 min 3. 60°C, 1:00 min 4. 72°C, 1:10 min 5. 72°C, 5:00 min (Steps 2-4 × 30)
KP42	oxy2	TGGTCTCCGTTACCATGTC	
KP43	kirOII_check_FW	GCGATTGGGGATCTTGGTGA	
KP44	kirOII_check_RV	ATGGAAACGGTGGTCACACG	
KP45	kirM_int-500bp_FW	CCACCCTGTCCGGTCGCGG	
KP46	kirM_int-500bp_RV	GCATCGTCCGCAGCCGCTG	1. 95°C, 3:00 min 2. 95°C, 0:30 min 3. 64°C, 0:30 min 4. 72°C, 2:30 min 5. 72°C, 5:00 min (Steps 2-4 × 40)
KP47	kirN_int-500bp_FW	GTGTTGCGGTGGAACCCCGG	
KP48	kirN_int-500bp_RV	GGGATCCTCCCCACCCGTG	
KP49	kirHIV_int-500bp_FW	CCTGGTGGAGGCCGACAACG	
KP50	kirHIV_int-500bp_RV	CGCCTCGGCGAGTTCGGCG	
KP51	kirHV_int-500bp_FW	GCATGAACTCCGTGCCCCAGG	
KP52	kirHV_int-500bp_RV	GCCGCCCGGTCAGTGCACG	
KP53	kirHVI_int-500bp_FW	TGGAGGAGTTCCTGGACCCCG	
KP54	kirHVI_int-500bp_RV	CGCCGTGATACAGACCGCCG	
KP55	kirOI_int-500bp_FW	CGAGGAAGGCGGACCCACCG	
KP56	kirOI_int-500bp_RV	GCGTCTCCCTCGGTGAAGTGGTG	
KP57	kirOII_int-500bp_FW	GACGGACCTCGTCGCCGGG	
KP58	kirOII_int-500bp_RV	GAGCTGGATCTGGCCGTCTTG	
KP59	pJet_check_FW	CGACTCACTATAGGGAGAGCGG C	
KP60	pJet_check_RV	AAGAACATCGATTTTCCATGGCA G	
KP61	pGM1190_seq_FW	CACGCGGAACGTCCGGG	
KP62	pGM1190_seq_RV	CCGCTGAAACTGTTGAAAGTTGT TTAGC	
KP63	pRM4_seq_FW	CAGTCACGACGTTGAAAACGAC GG	
KP64	pRM4_seq_RV	GGCACCGCGATGCTGTTGTG	

* 0:15 min for *kirHV*. 0:30 min for *kirM/kirHIV/kirHVI*. 0:45 min for *kirN/kirOI/kirOII*.

** 1:00 min for *kirM/kirHVI*. 1:30 min for *kirN/kirOI/kirOII*.

Table S3: HPLC-ESI-HRMS data for kirromycin and derivatives

Compound	RT (min)	m/z for [M-H] ⁻	Δm (ppm)	Chemical Formula	MS/MS fragment (m/z [M-H] ⁻)	MS/MS fragment (m/z [M+H] ⁺)
Kirromycin (1)*	12.2	795.4110	-2.6	C ₄₃ H ₆₀ N ₂ O ₁₂	499.2451	501.2578
20-O-demethyl-kirromycin (2, $\Delta kirM$)	11.2	781.3953	0	C ₄₂ H ₅₈ N ₂ O ₁₂	485.2292	487.2292
30-deoxy-kirromycin (3, $\Delta kirHVI$)	12.3	779.4177	2.3	C ₄₃ H ₆₀ N ₂ O ₁₁	499.2457	501.2586
5,6-dihydro-kirromycin (4, $\Delta kirOI$)	13.6	797.4286	1.6	C ₄₃ H ₆₂ N ₂ O ₁₂	501.2634	503.2768
30-hydroxy-5,6-dehydro-1-N-demethyl-16-deoxy-kirrothricin (5, $\Delta kirOII$)	13.5	763.4213	-2.7	C ₄₃ H ₆₀ N ₂ O ₁₀	467.2548	469.2698

* $\Delta kirN(kirHVI$ -complemented), $\Delta kirHIV$, and $\Delta kirHV$ had similar chromatograms and MS profiles to those of the wild type kirromycin (1), albeit production was lowered in $\Delta kirN(kirHVI$ -complemented).

Table S4: ¹H NMR spectra and assignments

¹H nuclear magnetic resonance (NMR) (**A**) and ¹³C NMR data (**B**) for 30-deoxy-kirromycin (**3**, kirromycin- Δ *kirHVI*), 5,6-dihydro-kirromycin (**4**, kirromycin- Δ *kirOI*), and 30-hydroxy-5,6-dehydro-1-*N*-demethyl-16-deoxy-kirrothricin (**5**, kirromycin- Δ *kirOII*) in CD₃OD at resonance frequency ¹600 resp. 150.8 MHz or ²700 resp. 176.1 MHz. The chemical shifts, obtained from NMR spectroscopy analysis, are represented by Δ ppm

	30-deoxy-kirromycin (3 , from $\Delta kirHVT$)		5,6-dihydro-kirromycin (4 , from $\Delta kirOI$)		30-hydroxy-5,6-dehydro-1-N-demethyl-16-deoxy-kirrothricin (5 , from $\Delta kirOII$)	
Position	δ_H [ppm] (Integral, Type, J in Hz) ²⁾	δ_C [ppm]	δ_H [ppm] (Integral, Type, J in Hz) ¹⁾	δ_C [ppm]	δ_H [ppm] (Integral, Type, J in Hz) ²⁾	δ_C [ppm]
1		-	-	-	-	-
2		164.5	-	n.d.	-	164.5
3	-	112.5	-	79.5 ⁰⁰	-	112.72 112.64
4	-	169.4	-	169.8	-	169.18, 169.01
5	6.11, 1H, s, br	102.1	2.54, 1H, dd, $J = 7.0$ (br)	37.3 (br) [#]	6.12, 1H, d, $J = 7.4$	102.0
6	7.39, 1H, br	137.8	3.42, 1H, m, $J = 7.0$ (br)	37.9	7.40, 1H, d, $J = 7.4$	137.8
7	-	198.9	-	n.d.	-	198.55, 198.63
8	-	141.4	-	138.8 ⁰⁰	-	142.9
9	6.94, 1H, br	142.5	6.20, m	134.3 ⁰⁰	6.97, 1H, ddd, $J = 11.4, 5.3, 1.2$	143.3
10	6.69, 1H, b, dd, $J = 12.5, 12.5$	129.4	6.56, m ⁰⁰	129.3	6.73, 1H, dd, $J = 11.4, 14.7$	129.5
11	6.07, 1H, dd, $J = 15.1, 7.2$	137.0	6.56, m ⁰⁰	137.2 ⁰⁰	6.67, 1H, d, $J = 14.7, 10.7$	142.3
12	6.45, 1H, dd, $J = 15.0, 11.0$	133.6	6.40, 1H, $J = 11.5, 15.0$	133.9 (br)	6.61, 1H, dd, $J = 14.7, 10.7$	142.5
13	6.52, 1H, m (with 24)	136.1	5.99, m	135.1 (br)	6.46, 1H, dd, $J = 10.5, 5.9$ 6.44, 1H, dd, $J = 10.6, 5.7$	138.7 134.0
14	4.31, 1H, m	81.6	4.25, 1H, dd, $J = 12.5$	81.8	6.37, 0.6 H, dd, $J = 14.7, 10.5$	132.1
15	4.32, 1H, m	75.0	4.28, 1H, dd, $J = 12.5$	75.0	5.90, 0.4 H, dt, $J = 14.9, 7.4$; 6.26, 0.6H dd, $J = 14.8, 10.4$ (also 6.21, dd, $J = 11.3, 11.3, 5.67, m,$; 6.78, m)	136.02 133.50 (131.1, 132.2, 133.5)
16	4.19, 1H, dd, $J = 4.4$	74.0	4.17, 1H, dd, $J = 4.4$	74.0	2.25, m 2.40, m 2.43, m	40.0, 40.7, 34.8

	30-deoxy-kirromycin (3 , from $\Delta kirHVT$)		5,6-dihydro-kirromycin (4 , from $\Delta kirOI$)		30-hydroxy-5,6-dehydro-1-N-demethyl-16-deoxy-kirrothricin (5 , from $\Delta kirOII$)	
Position	δ_H [ppm] (Integral, Type, J in Hz) ²⁾	δ_C [ppm]	δ_H [ppm] (Integral, Type, J in Hz) ¹⁾	δ_C [ppm]	δ_H [ppm] (Integral, Type, J in Hz) ²⁾	δ_C [ppm]
17	3.71, 1H, dd, $J=7.3, 4.1$	85.0	3.68, 1H, dd, $J=4.0, 7.5$	84.9	4.06, 1H, m	70.9
18	-	-	-	-	-	-
19	2.20, 1H, m	36.8	2.16, 1H, ddq, $J=2.0, 7.0$	36.8	1.69, 1H, m	40.8
20	3.34, 1H, d, 9.2	91.9	3.32, s	91.9	3.46, 1H, d, $J=10.1$	90.0
21	-	136.1	-	136.0	-	136.7
22	5.69, 1H, dd, $J=15.0, 6.0$	130.8	5.96, 1H, d (br), $J=10$	130.9	5.99, 1H, d, $J=10.5$	130.4
23	6.56, 1H, dd, $J=15.2, 11.0$	128.0	6.49, 1H, m, $J=11.0, 16.0$	128.3	6.51, 1H, dd, $J=15.2, 11.0$	128.3
24	6.53, 1H, dd, $J=15.2, 11.0$	128.2	5.67, 1H, m, $J=6.0, 16.0$	131.0	5.66, 1H, m (with 35)	130.6
25a	3.90, 1H, dd, $J=15.8, 5.8$	42.0	3.86, 1H, dd, $J=6.5, 15.0$	42.0	3.89, 1H, dd, $J=15.8, 5.5$	42.1
25b	3.95, 1H, dd, $J=15.8, 5.9$		3.93, 1H, dd, $J=6.5, 15.0$		3.95, 1H, dd, $J=15.8, 6.7$	
26-N	-	-	-	-	-	-
27	-	176.9	-	177.9	-	177.9
28	2.39, 1H, dd, $J=11.1, 4.2$	58.3	2.82, 1H, dd, $J=4.0, 11.0$	52.5	2.84, 1H, dd, $J=11.0, 4.5$	52.5
29	-	99.5	-	101.0	-	101.0
30	1.95, 1H, dd, $J=12.6, 4.6$ 1.48, 1H, dd, $J=12.6, 12.5$	38.3	3.65, 1H, d, $J=4.0$	71.4	3.68, 1H, d, $J=3.6$	71.4
31	3.74, 1H, d, $J=12.5, 4.6$	72.6	3.57, 1H, d, $J=4.0$	74.0	3.60, 1H, d, $J=3.6$	74.0
32	-	40.3	-	40.0	-	39.9
33	4.17, 1H, d, $J=6.0$	77.7	4.21, 1H, d, $J=6.0$	77.3	4.24, 1H, t, $J=5.8$	77.3
34-O	-	-	-	-		
35	5.64, 1H, m (with 24)	130.3	5.62, 1H, dd, $J=6.0, 15.0$	130.5	5.66, 1H, m (with 24)	130.6
36	6.55, 1H, m (with 24)	127.9	6.54, m	127.7	6.58, 1H, dd, $J=14.8, 11.8$	127.7
37	6.01, 1H, ddd, $J=10.8, 10.8,$	130.4	5.99, m	130.6	6.01, 1H, ddd, $J=10.8, 10.8, 1.5$	130.5

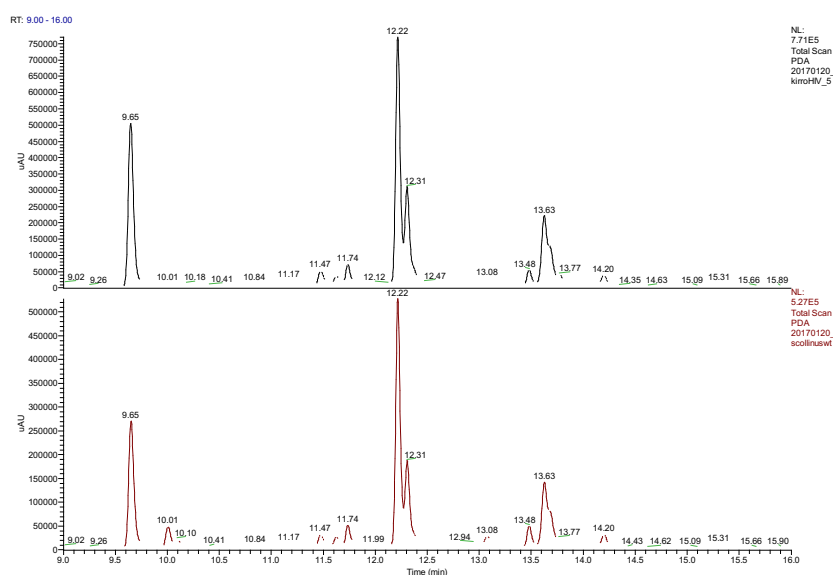
	30-deoxy-kirromycin (3 , from $\Delta kirHVT$)		5,6-dihydro-kirromycin (4 , from $\Delta kirOI$)		30-hydroxy-5,6-dehydro-1-N-demethyl-16-deoxy-kirrothricin (5 , from $\Delta kirOII$)	
Position	δ_H [ppm] (Integral, Type, J in Hz) ²⁾	δ_C [ppm]	δ_H [ppm] (Integral, Type, J in Hz) ¹⁾	δ_C [ppm]	δ_H [ppm] (Integral, Type, J in Hz) ²⁾	δ_C [ppm]
	1.0					
38	5.49, 1H, dq, $J = 11.0, 6.9$	126.5	5.44, 1H, dq, $J = 7.0, 11.0$	126.4	5.49, 1H, dq, $J = 11.0, 7.0$	126.4
39	1.77, 3H, dd, $J = 7.1, 1.5$	13.7	1.73, 3H, dd, $J = 2.0, 7.0$	13.7	1.77, 3H, dm, $J = 7.0$	13.7
40	2.01, 3H,	11.7	1.95, s (br)	14.4 (br)	2.00, 2.04, 3H, d, $J = 0.9$	11.61, 11.68
41	0.84, 3H, d, $J = 6.8$	13.9	0.81, 1H, d, $J = 7.0$	13.9	0.69, 3H, d, $J = 7.0$	9.49, 9.57
42	3.18, 3H, s	56.2	3.15, 3H, s (sh)	56.2	3.17, 3H, s	56.32
43	1.69, 3H, s	11.2	1.66, 3H, s (sh)	11.2	1.63, 3H, s	11.0 (sh)
44	1.73, 2H, m	21.6	1.70, m	21.1	1.73, 2H, m	21.1
45	0.95, 3H, t, $J = 7.3$	12.4	0.92, 3H, t, $J = 7.5$	12.3	0.95, 3H, t, $J = 7.4$	12.3
46	0.77, 3H, s	12.4	0.89, 3H, s ⁰⁰	15.9	0.92, 3H, s	15.9
47	0.94, 3H, s	23.0	0.89, 3H, s ⁰⁰	24.6	0.92, 3H, s	24.6

*: ¹³C shift determined by HSQC or HMBC. #: assigned due to HSQC correlations. ⁰⁰: not unambiguously assigned due to tautomerization, missing 2D correlations, or overlaying signals. n.d.: not detected. n.a.: not assigned.

Figure S1-I – S1-II: UV-VIS profiles of $\Delta kirHIV$ and $\Delta kirHV$ mutants

The $\Delta kirHIV$ and $\Delta kirHV$ mutants were grown in parallel with *Streptomyces collinus* Tü 365 (wild type) in kirromycin production medium and extracted with ethyl acetate. The extracts were dried, dissolved in methanol, and analysed using HPLC-ESI-HRMS. The recorded UV profiles of $\Delta kirHIV$ (I) and $\Delta kirHV$ (II) (black chromatograms) were similar to those of the wild type (red chromatograms). These results indicate that the two genes *kirHIV* and *kirHV* are not directly involved in the biosynthesis of kirromycin. In the case of $\Delta kirHV$ (II), we suspect that the lower intensity of the peak at 12.3 min (compared to the wild type) could be explained from almost complete conversion of the pathway intermediate into kirromycin.

(I)



(II)

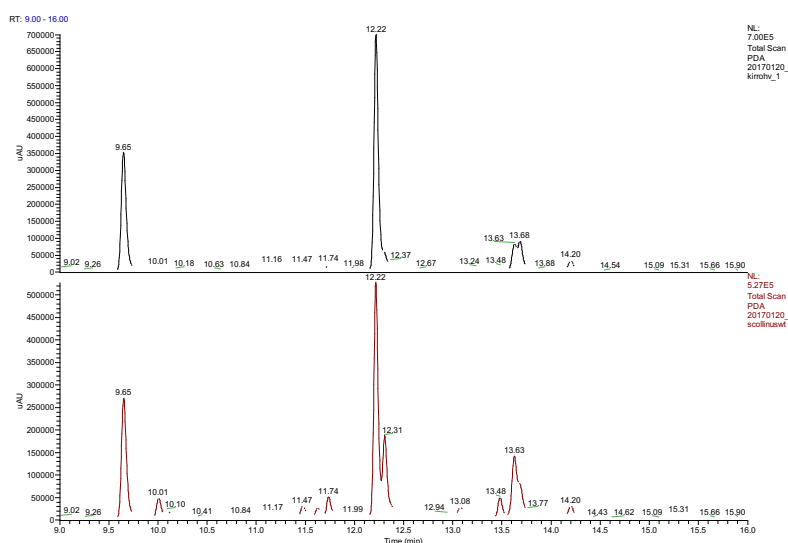
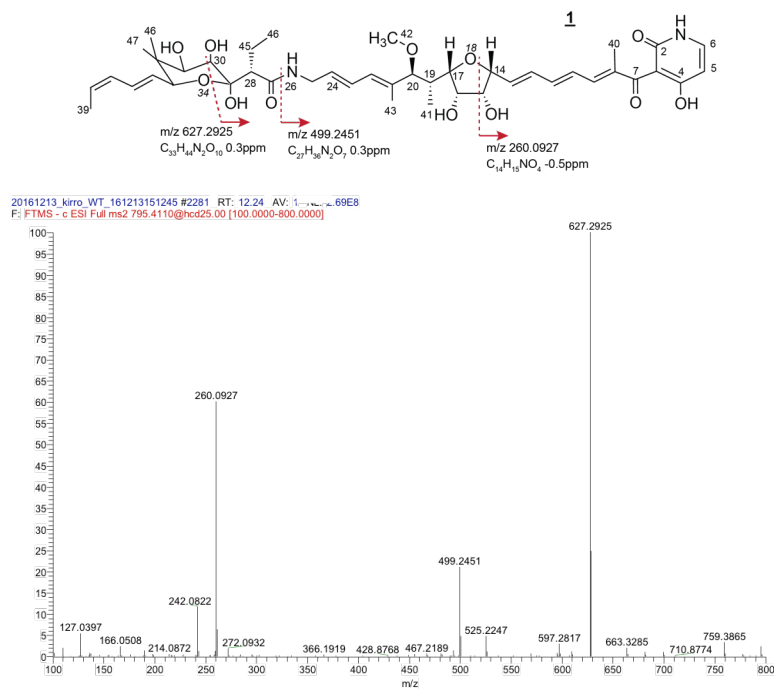


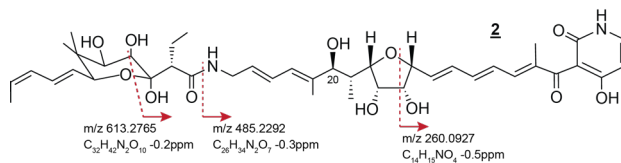
Figure S2-I – S2-V: MS/MS spectra of kirromycin and derivatives

MS/MS spectra for **(I)** kirromycin (**1**), **(II)** 20-*O*-demethyl-kirromycin (**2**), **(III)** 30-deoxy-kirromycin (**3**), **(IV)** 5,6-dihydro-kirromycin (**4**), and **(V)** 30-hydroxy-5,6-dehydro-1-*N*-demethyl-16-deoxy-kirrothricin (**5**). Recorded in negative mode (ESI-) with higher-energy collisional dissociation (HCD) of 25 eV.

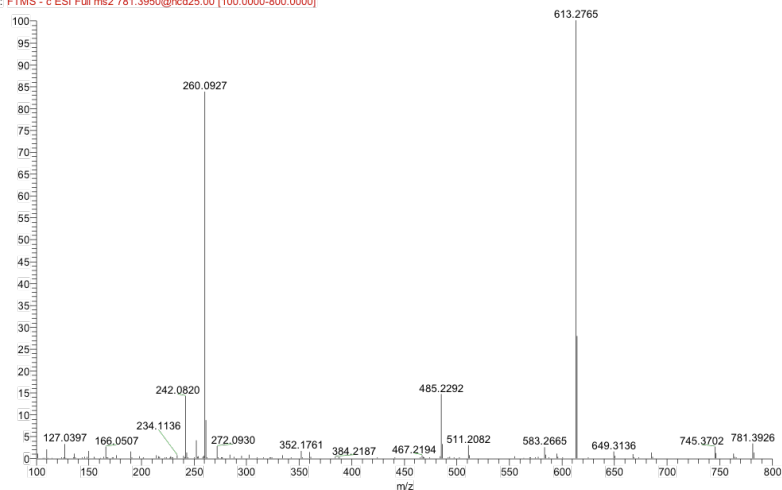
(I)



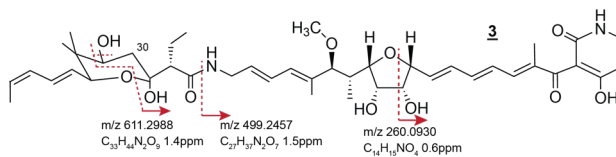
(II)



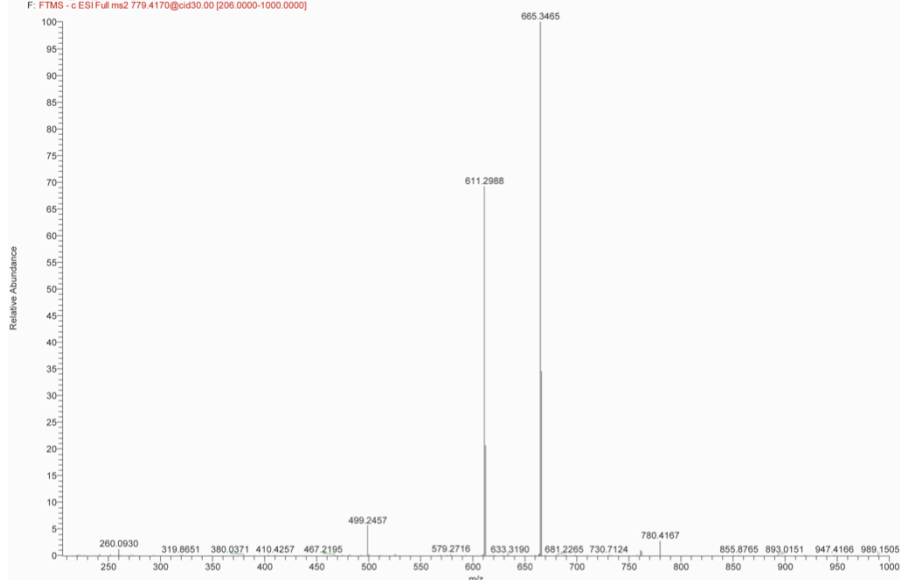
20161213_kirra_kirM_161213154449_#1678 RT: 11.12 AV: 1.19E8
F: FTMS - c ESI Full me2 781.3950@rcd25.00 [100.0000-800.0000]



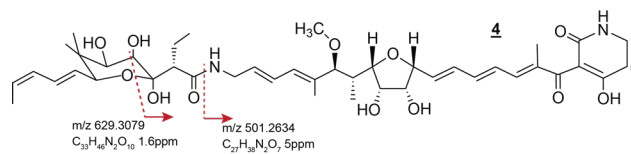
(III)



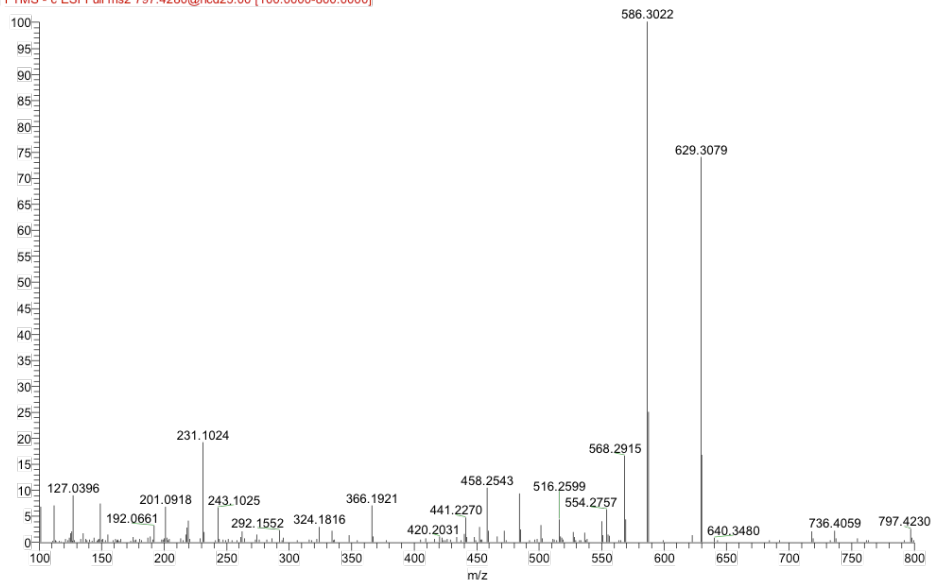
20161202_kirra_kirMvineg_#471 RT: 12.48 AV: 1 NL: 1.20E8
F: FTMS - c ESI Full me2 779.4170@cs430.00 [206.0000-1000.0000]



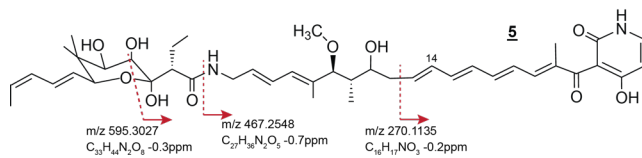
(IV)



20161213_kirro-OI_161213164855 #2839 RT: 13.67 AV: 1J9E8
F: FTMS - c ESI Full ms2 797.4280@hcd25.00 [100.0000-800.0000]



(V)



20161213_kirro-OI_161213172057 #2616 RT: 13.48 AV: 185E8
F: FTMS - c ESI Full ms2 763.4210@hcd25.00 [100.0000-800.0000]

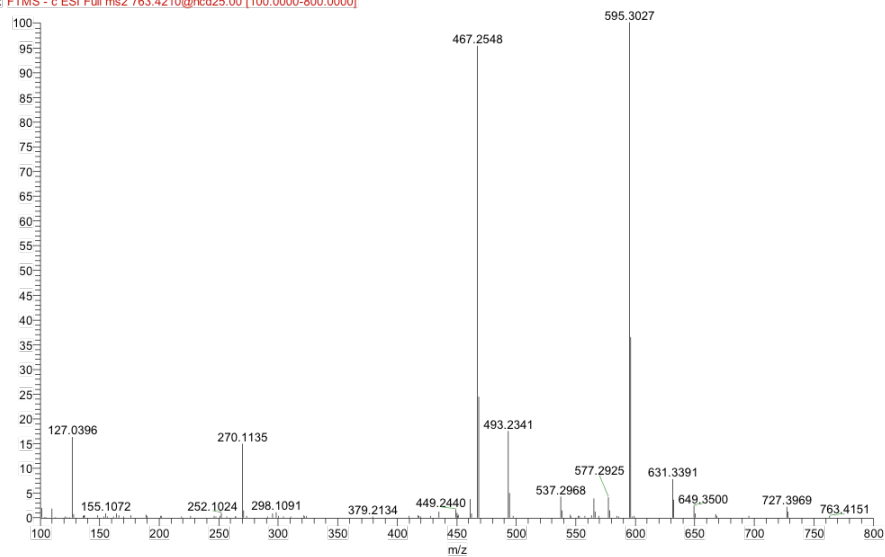
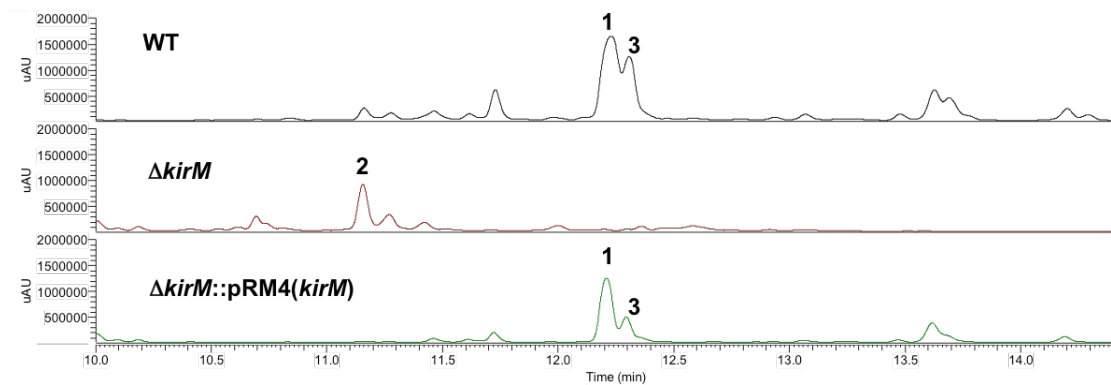


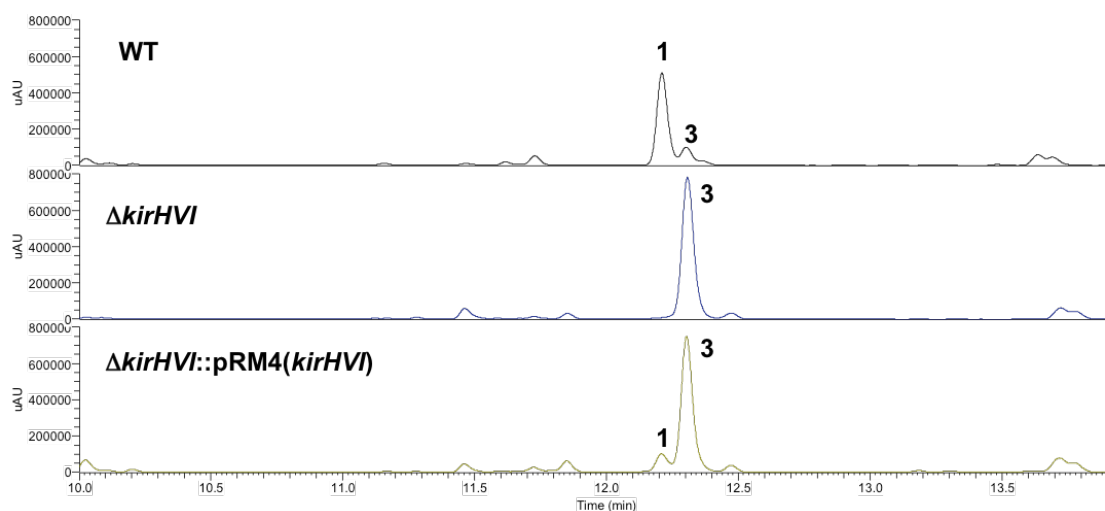
Figure S3-I – S3-VI: HPLC-ESI-UV-Vis profiles of the wild type (WT), Δkir mutants, and complemented mutants

UV-Vis profiles of *Streptomyces collinus* Tü 365 (WT) compared to mutants (I) $\Delta kirM$, (II) $\Delta kirHVI$, (III) $\Delta kirOI$, and, (IV) $\Delta kirOII$, along with their respective complementations. The $\Delta kirN$ mutant and its single (*kirHVI*) and double (*kirN+HVI*) complementations are shown in (V) and (VI), respectively.

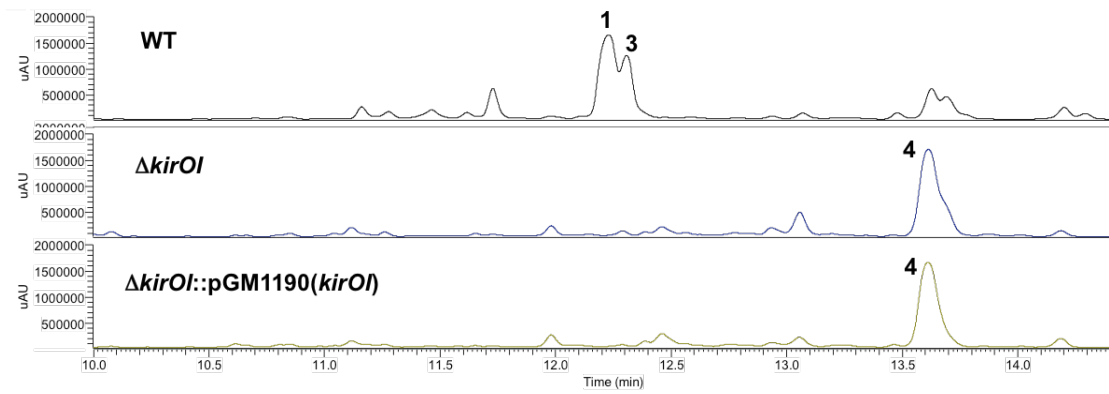
(I)



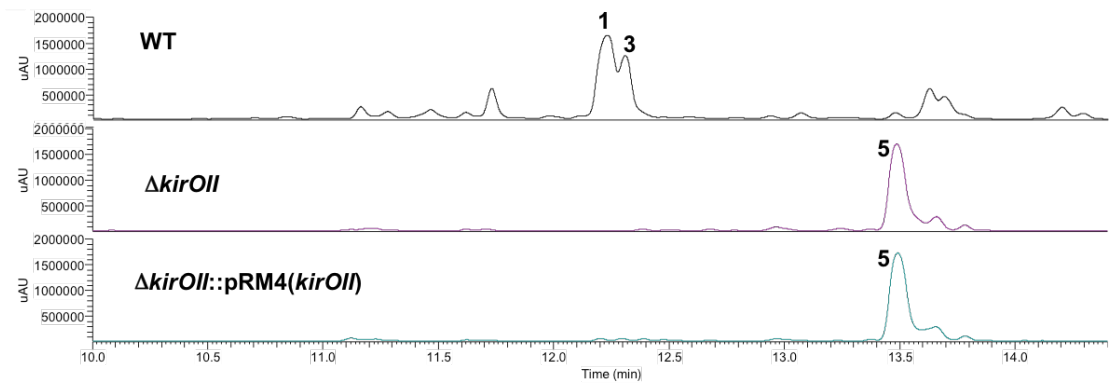
(II)



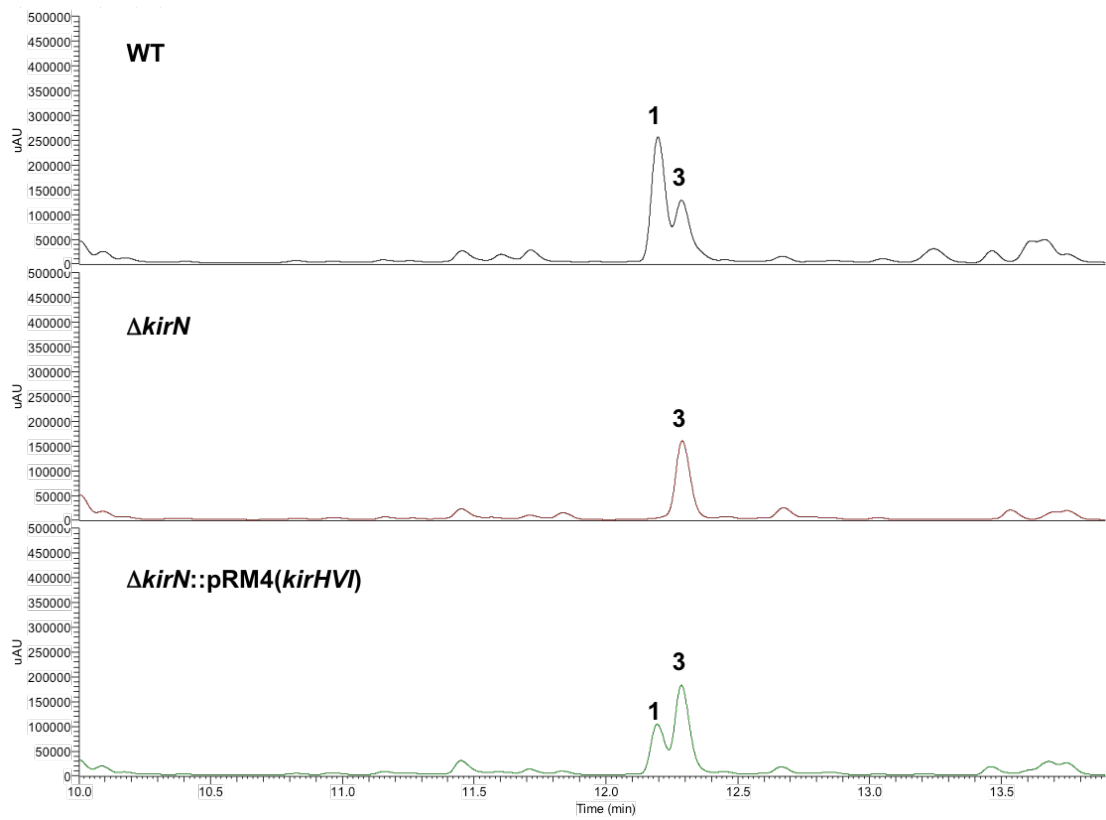
(III)



(IV)



(V)



(VI)

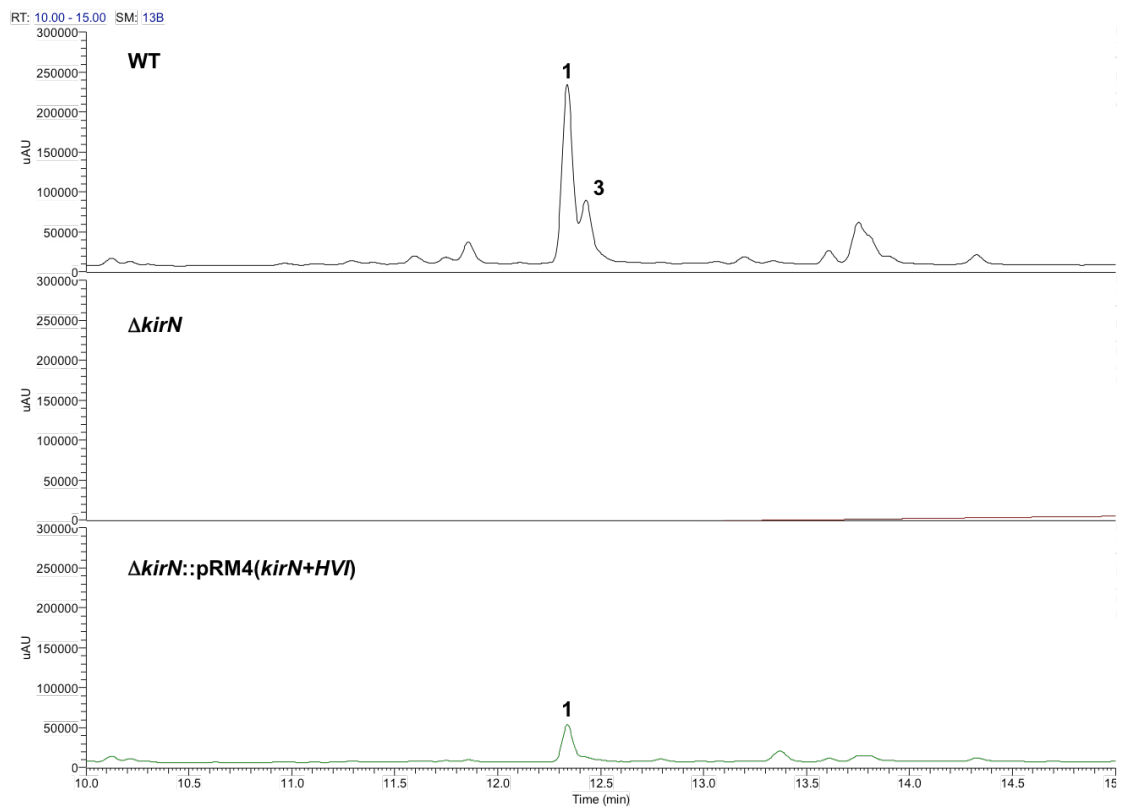
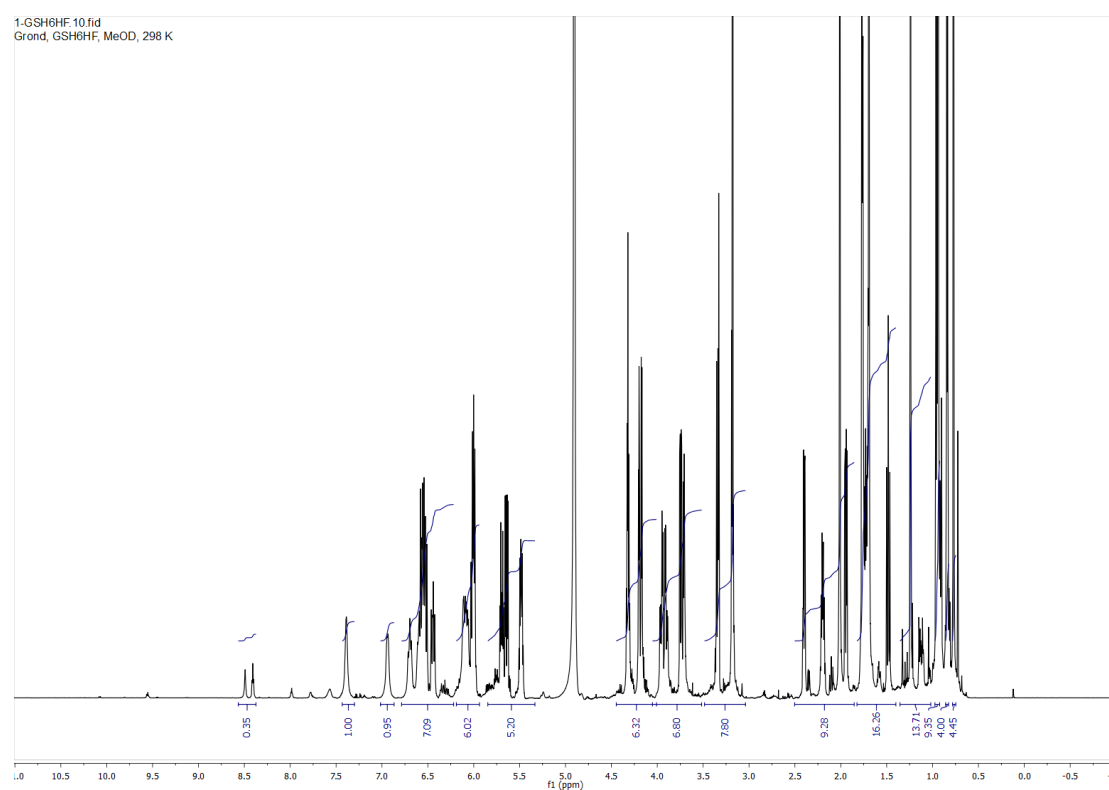


Figure S4-I – S4-III: ^1H NMR and ^{13}C NMR data and assignment for 30-deoxy-kirromycin (3), 5,6-dihydro-kirromycin (4), and 30-hydroxy-5,6-dehydro-1-*N*-demethyl-16-deoxy-kirrothricin (5)

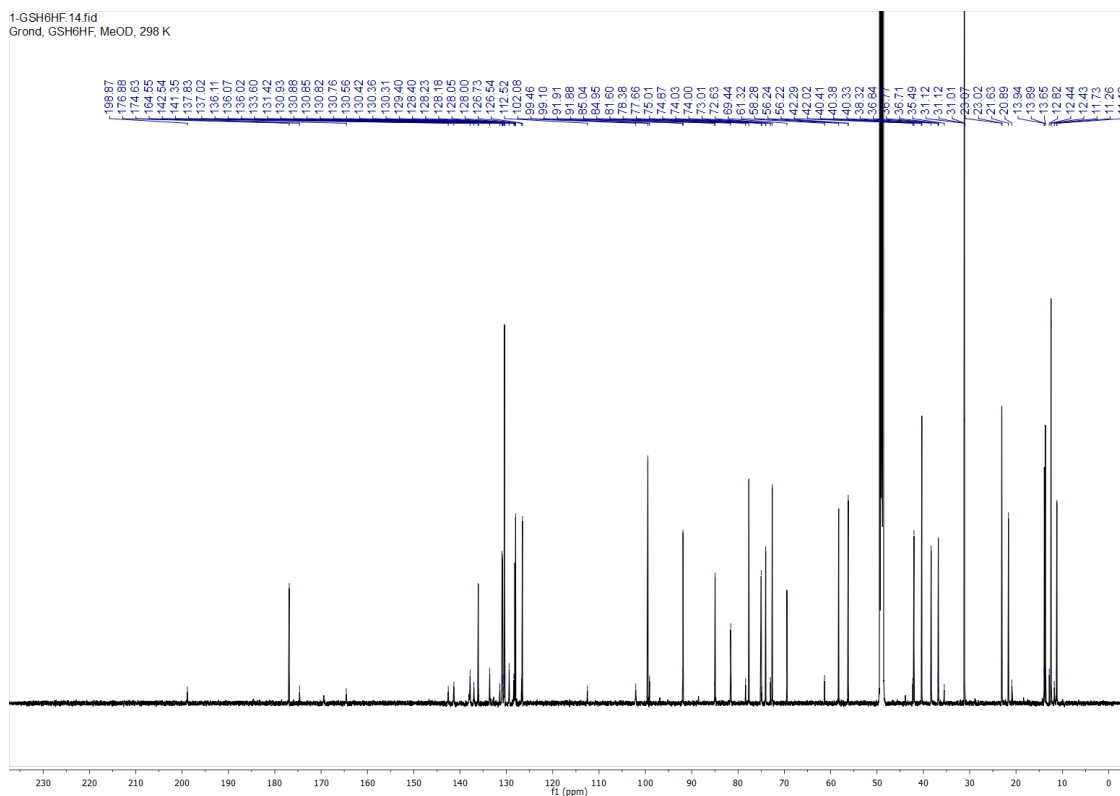
(A) ^1H NMR and (B) ^{13}C NMR of (I) 30-deoxy-kirromycin (3), (II) 5,6-dihydro-kirromycin (4), and (III) 30-hydroxy-5,6-dehydro-1-*N*-demethyl-16-deoxy-kirrothricin (5) (CD_3OD , 298 K). Resonance frequency 1 600 resp. 150.8 MHz, 2 700 resp. 176.1 MHz.

(IA) ^1H NMR spectrum of 3



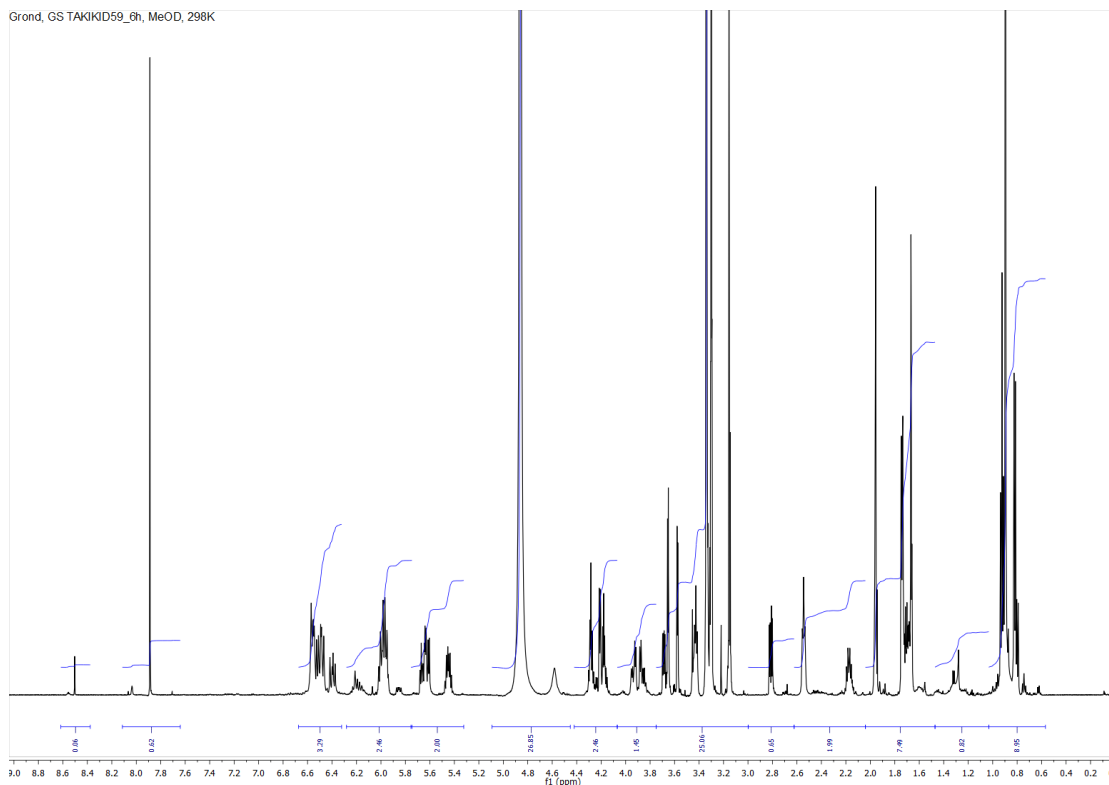
(IB) ^{13}C NMR spectrum of 3

1-GSH6HF_14.fid
Grond, GSH6HF, MeOD, 298 K

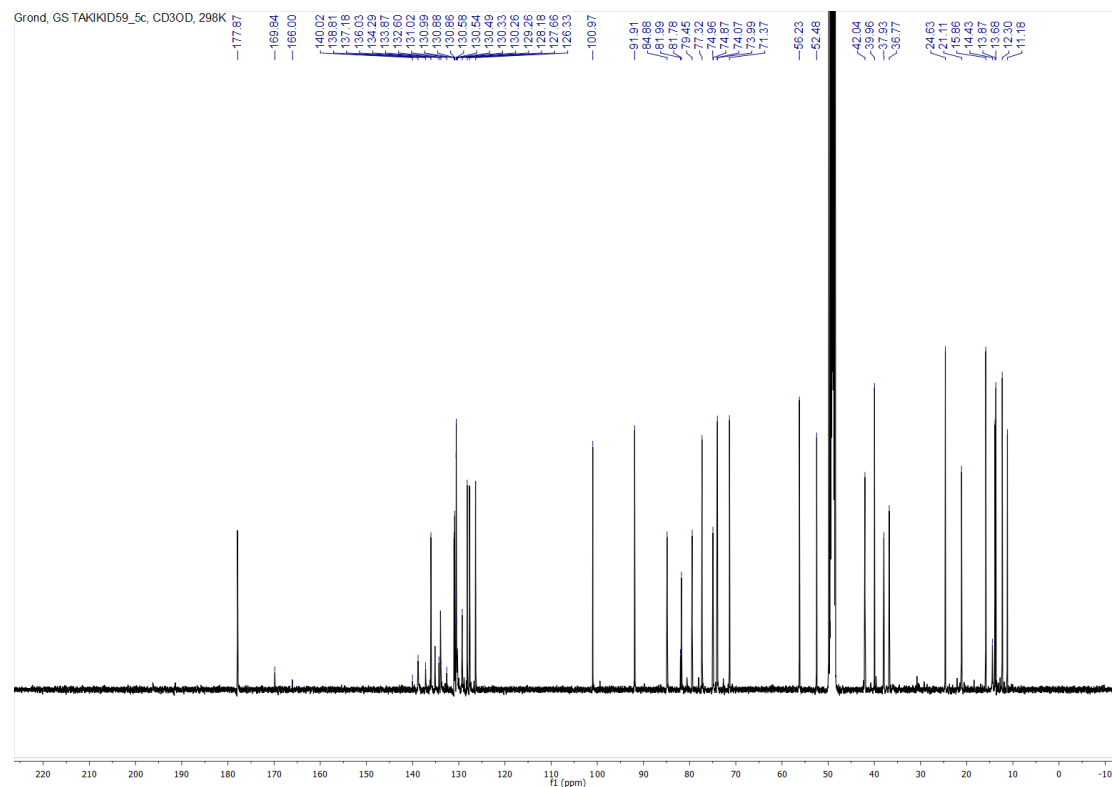


(IIA) ^1H NMR spectrum of 4

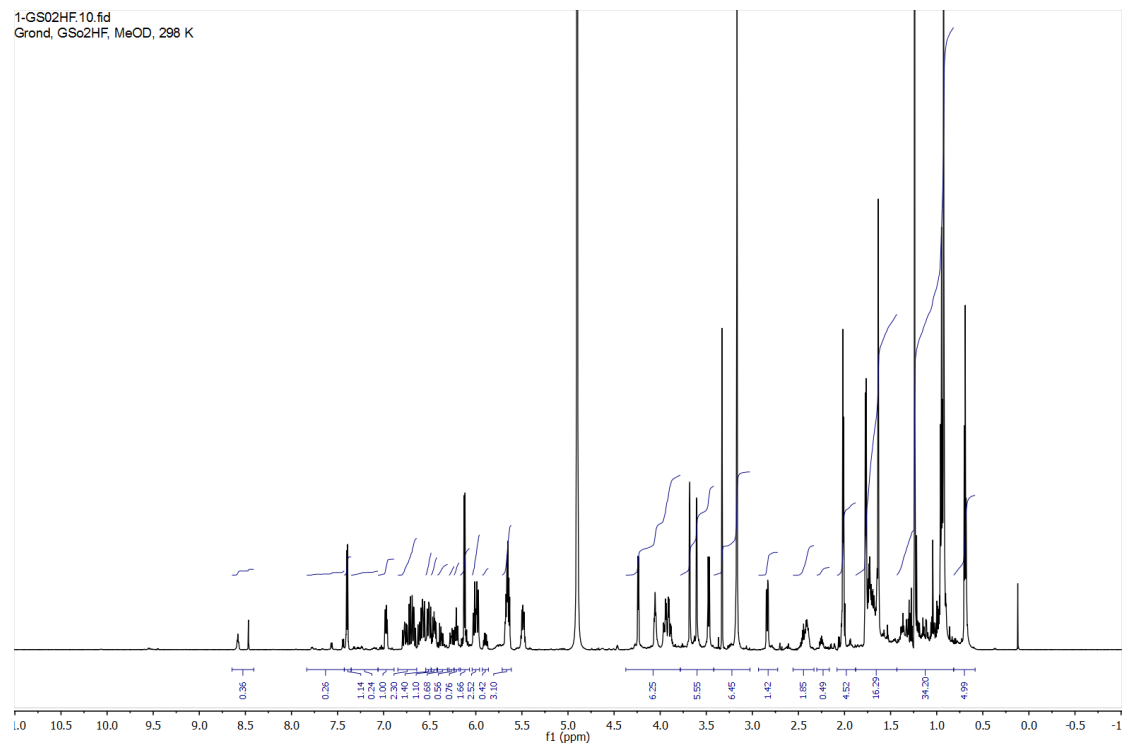
Grond, GS TAKIKID59_gh, MeOD, 298K



(IIB) ^{13}C NMR spectrum of 4



(IIIA) ^1H NMR spectrum of 5



(IIB) ¹³C NMR spectrum of 5

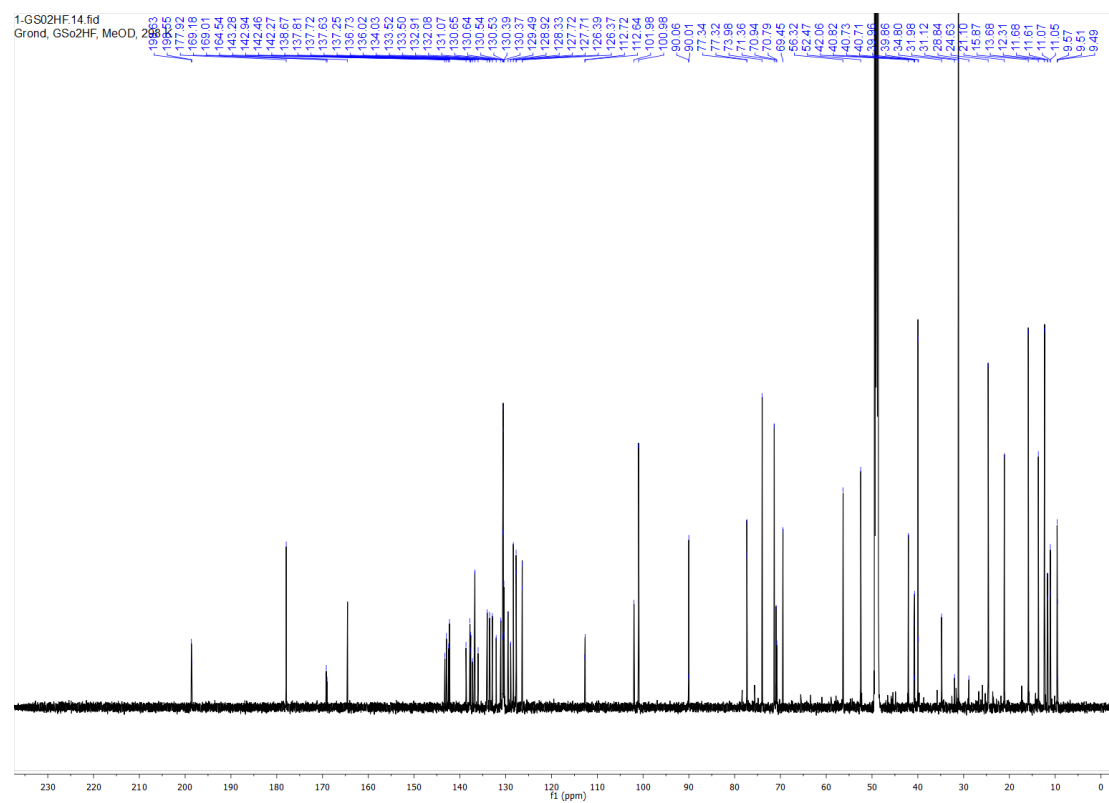
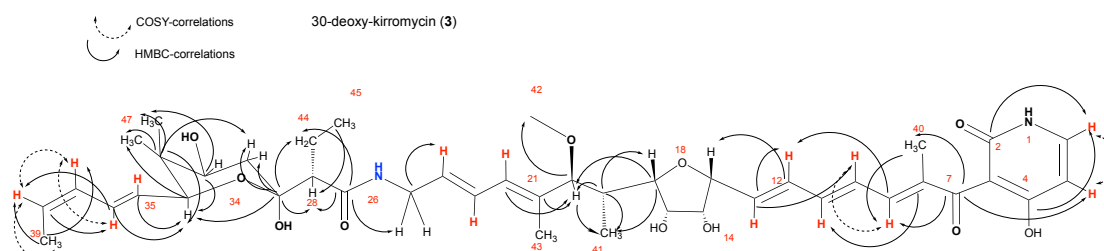


Figure S5-I – S5-III: 2D-NMR of 30-deoxy-kirromycin (3), 5,6-dihydro-kirromycin (4), and 30-hydroxy-5,6-dehydro-1-*N*-demethyl-16-deoxy-kirrothricin (5)

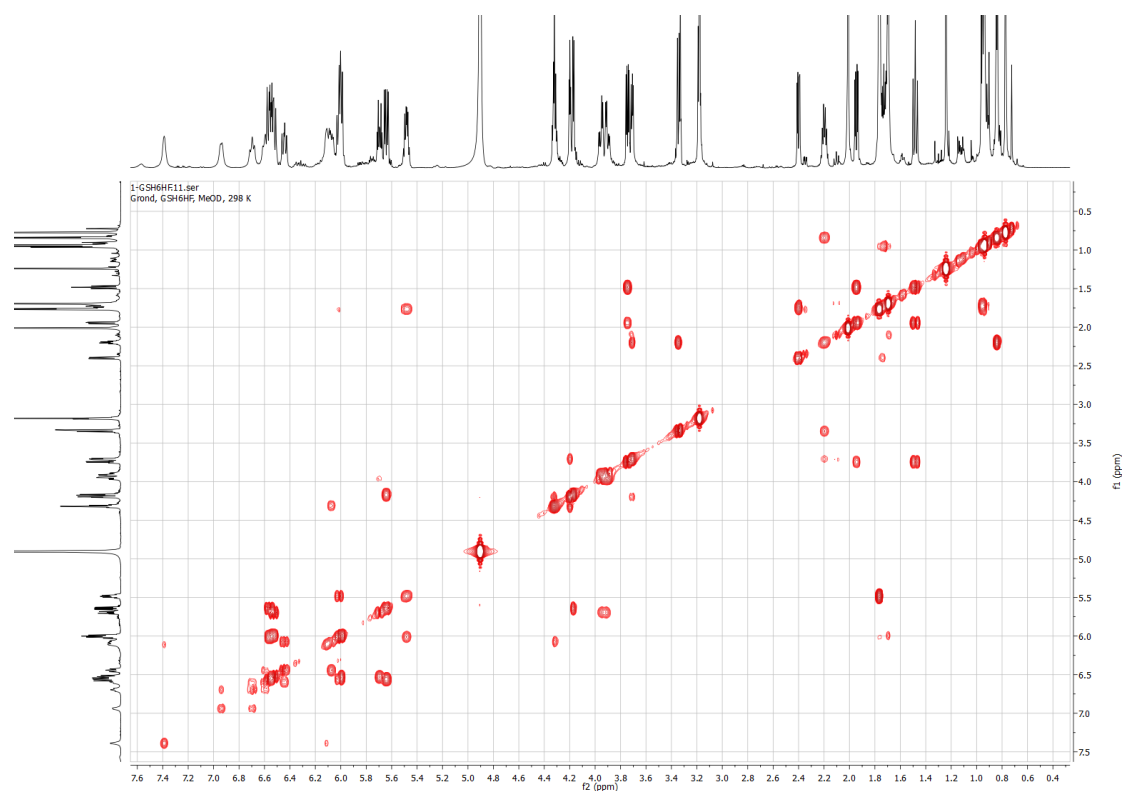
(I) 30-deoxy-kirromycin (3)

Homonuclear Correlation Spectroscopy (COSY) underlined the partial structure for the 30-deoxygenated pyran ring in 30-deoxy-kirromycin (**3**) (**IA** and **ID**), which was isolated from the $\Delta kirHVI$ mutant. It lacked the C-30-hydroxy group as had been found previously for the heneicomycin analogue⁹. The signal for H-30_a (δ 1.48) showed strong cross correlation with the H-30_b (δ 1.95), and both exhibited further correlations with H-31 (δ 3.74). (**IB**) The Heteronuclear Single Quantum Correlation (HSQC) gave evidence to the CH₂-connectivity for both H-30_a and H-30_b connection attached to one carbon atom (C-30, (d_C = 38.3). (**IC**) The Heteronuclear Multiple Bond Correlation (HMBC) spectrum showed correlations between H-30_a (δ 1.48), H-30_b (δ 1.95) and C-29 (δ 99.5) and corroborated the 30-deoxy ring in **3**.

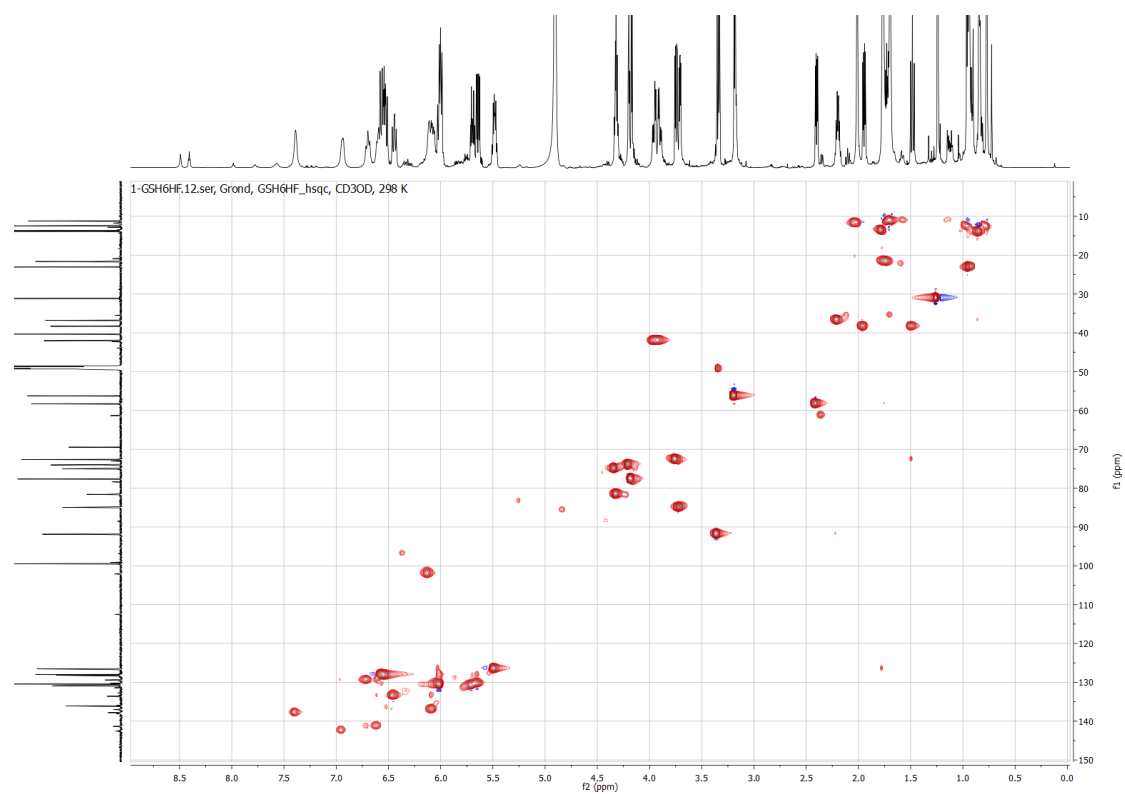


Formula S5-I Selected COSY (double dashed arrowed), TOCSY (dashed line), and HMBC (single arrowed) correlations for 30-deoxy-kirromycin (**3**).

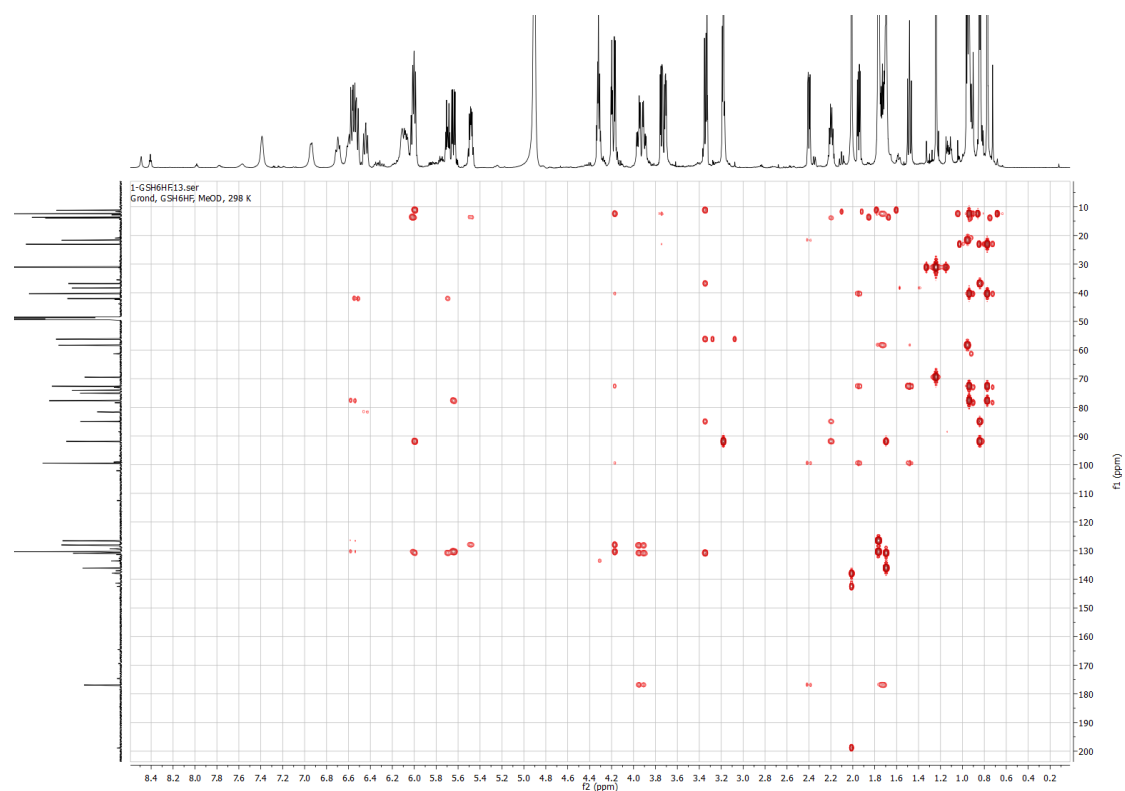
(IA) H-H-correlation (COSY) spectrum of 30-deoxy-kirromycin (3)



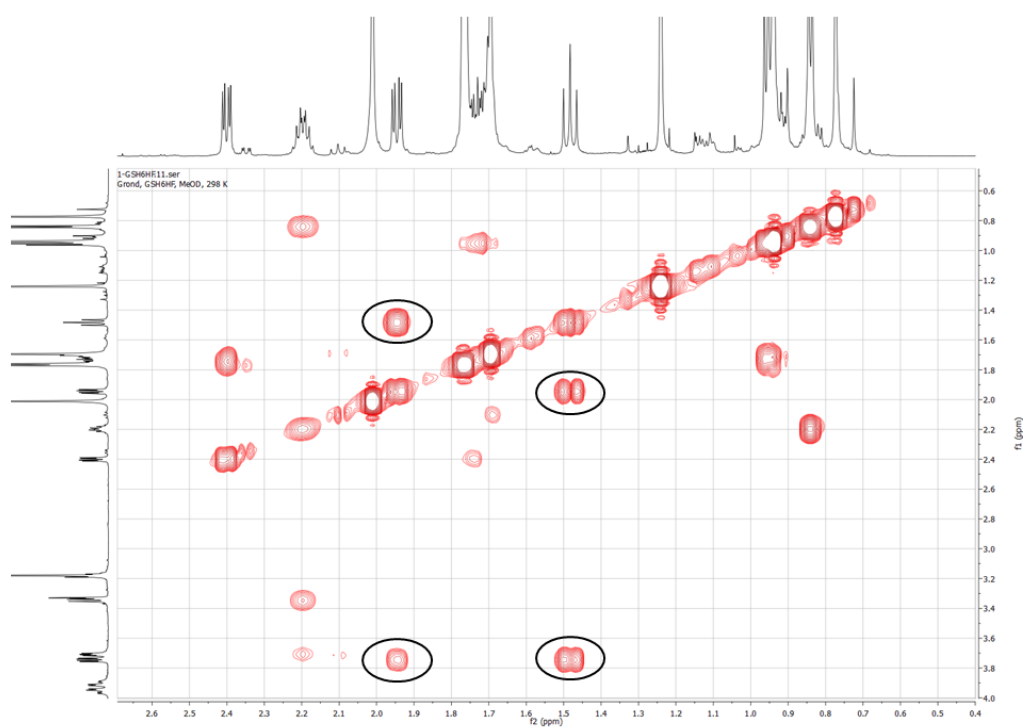
(IB) CH-correlation (HSQC) spectrum of 30-deoxy-kirromycin (3)



(IC) Multiple bond CH-correlation (HMBC) spec. of 30-deoxy-kirromycin (3)

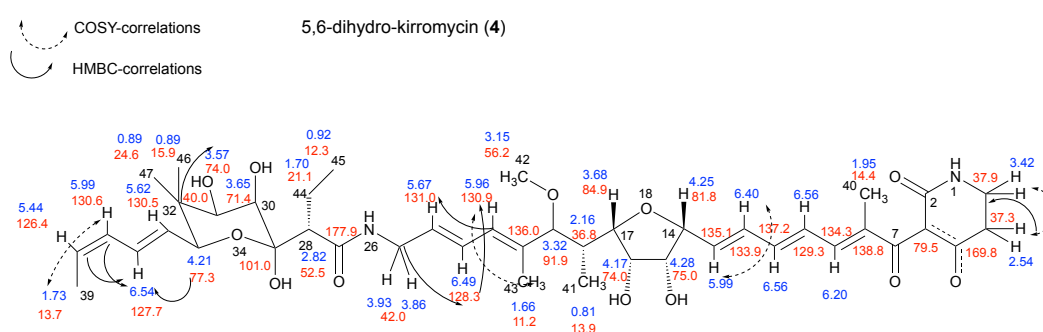


(ID) Key correlations highlighted for 30-deoxy-kirromycin (3)



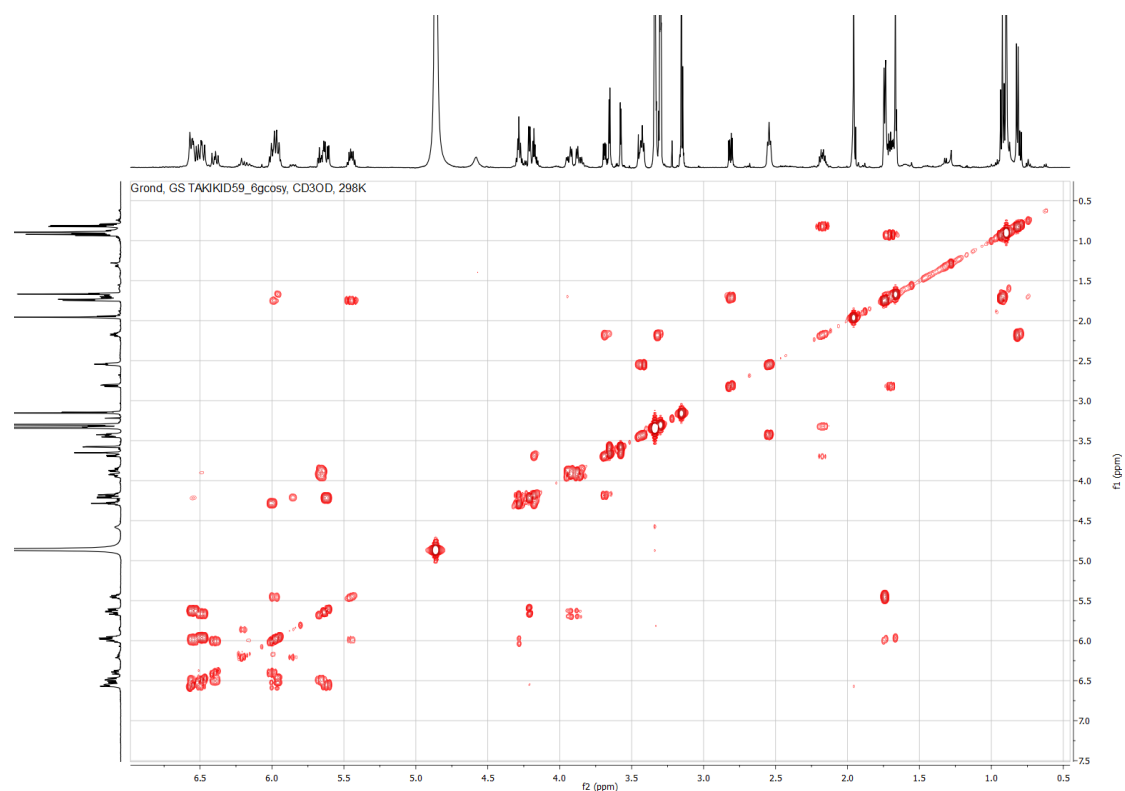
(II) 5,6-dihydro-kirromycin (4)

(IIA) In addition to the one-dimensional ^1H NMR spectra, the COSY spectrum gave evidence for the two additional methylene groups 5- H_2 (δ 2.54, t, broad) and 6- H_2 (δ 3.42, t, broad) with strong correlation signals (IIA and IID) for the 5,6-dihydro-kirromycin (4), isolated from the ΔkirOI mutant. (IIB) The HSQC gave evidence for the C-H connectivity. (IIC) The HMBC spectrum showed significant correlations of the intact kirromycin triene conjugated double bonds, e.g. 22-H (δ 5.96) with C-19 (δ_{C} 91.9) and C-43 (δ_{C} 11.2) and C-23 (δ_{C} 128.3) and, in addition, the correlation of 33-H (δ 4.21) with C-36 (δ_{C} 127.7).

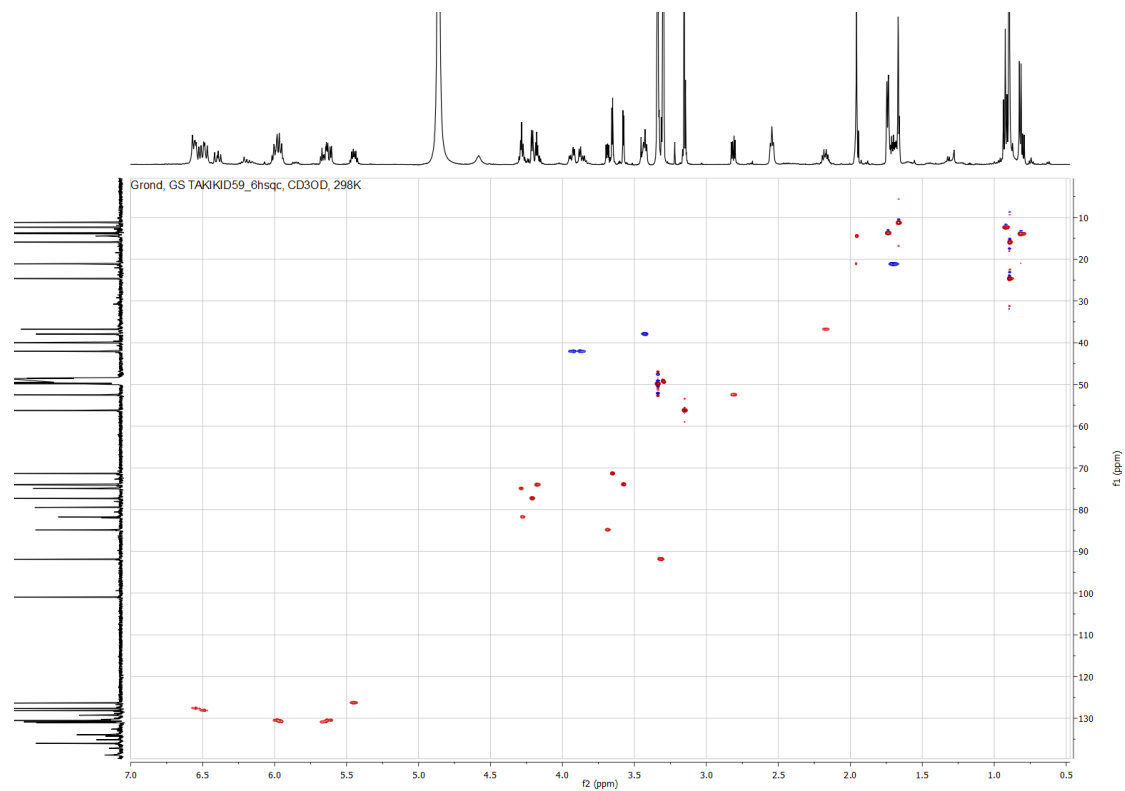


Formula S5-II Full assignment of ^1H and ^{13}C NMR data as example and selected COSY (double dashed arrowed) and HMBC (single arrowed) correlations for 5,6-dihydro-kirromycin (4).

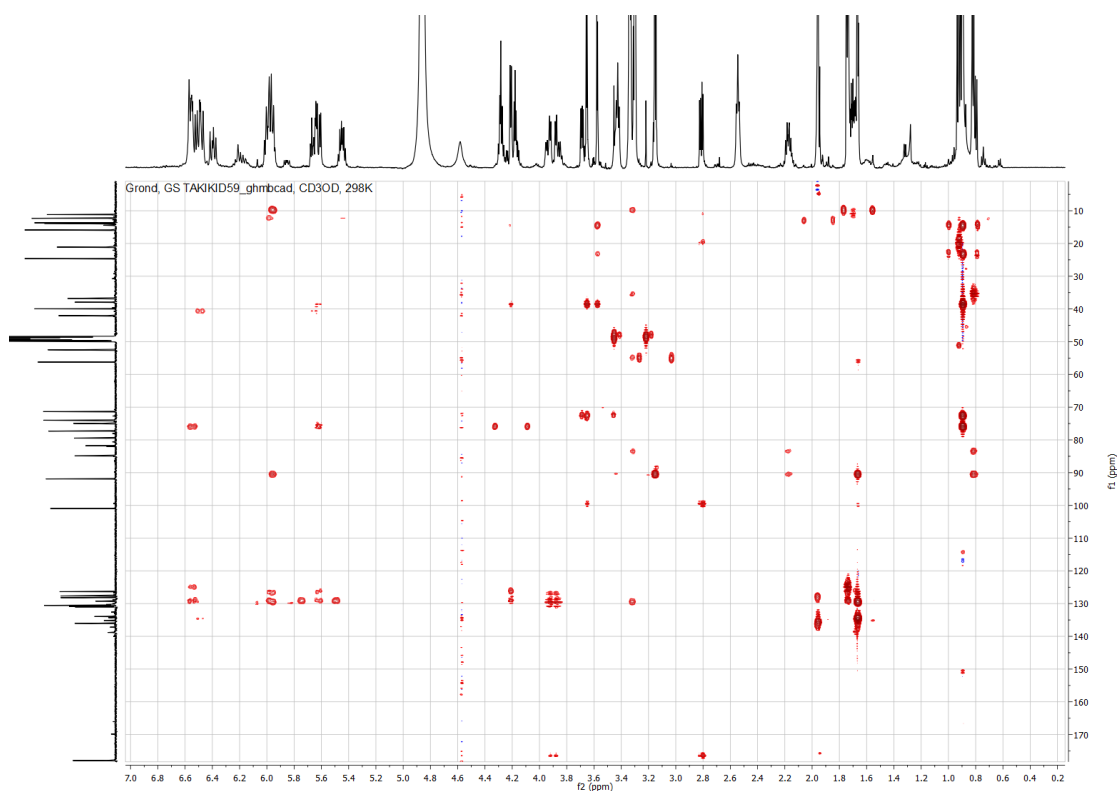
(IIA) H-H-correlation (COSY) spectrum of 5,6-dihydro-kirromycin (4)



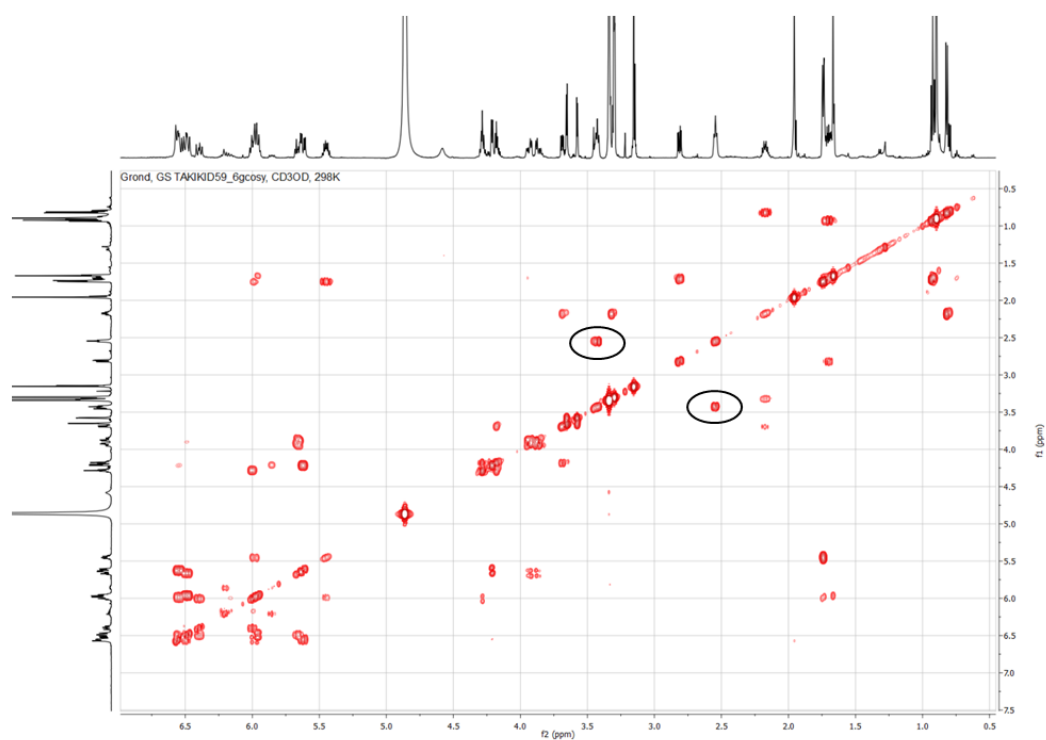
(IIB) CH-correlation (HSQC) spectrum of 5,6-dihydro-kirromycin (4)



(IIC) Multiple bond CH-correlation (HMBC) spec. of 5,6-dihydro-kirromycin (4)

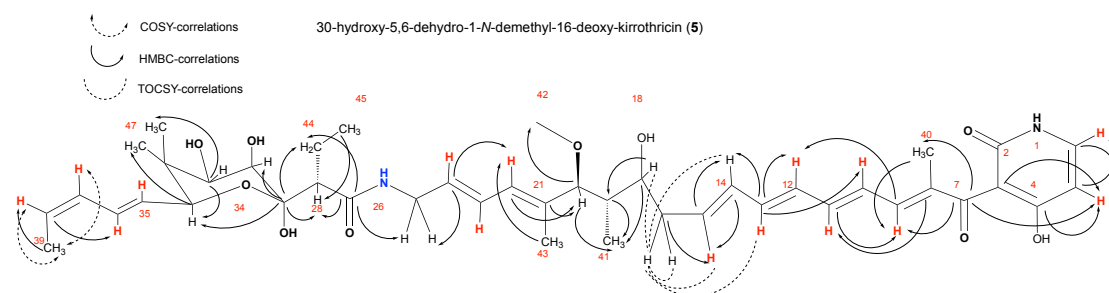


(IID) Key correlations highlighted for 5,6-dihydro-kirromycin (4)



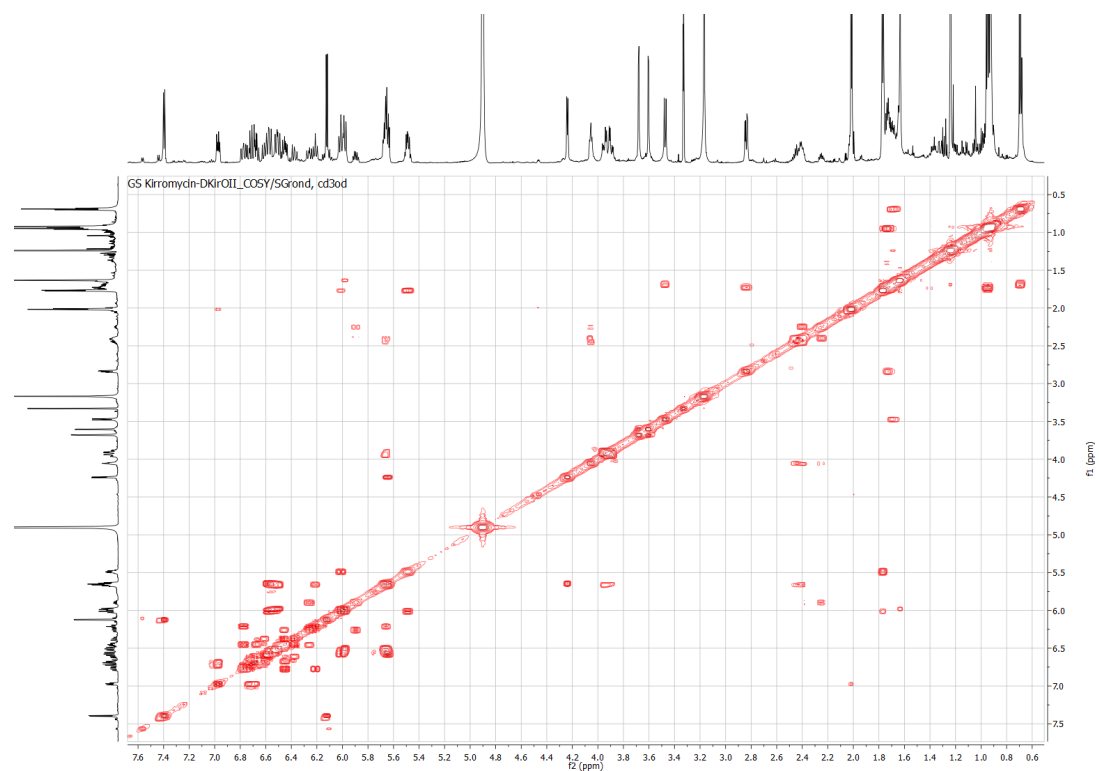
(III) 30-hydroxy-5,6-dehydro-1-*N*-demethyl-16-deoxy-kirrothricin (5)

COSY and Total Correlated Spectroscopy (TOCSY) spectra established the partial structure for the disrupted furan part (III A) in the 30-hydroxy-5,6-dehydro-1-*N*-demethyl-16-deoxy-kirrothricin (5) derivative isolated from the $\Delta kirOII$ mutant. H-17 (δ 4.06) exhibited correlations with both H-19 (δ 1.69) and H-16 (δ 2.40, 2.43, δ 2.25). H-16 exhibited further correlations to an olefinic proton H-15 (δ 5.90, 6.26), which confirmed the location of the extra double bond. (II) The HSQC gave evidence to the C-H connectivity. (III) The HMBC spectrum showed correlations between H-17 (δ 4.06), CH₃-41, C-16 (δ 40.0) and C-20 (δ 90.0), and corroborated the final structure of 5. The new kirrothricin-like tetraene fragment was readily assigned from the HMBC-correlations of the CH-groups of C-9 to C-15 (see Formula S5-III). The red shifted UV-Vis spectrum for 5 could be explained by the elongation of the double bond chain.

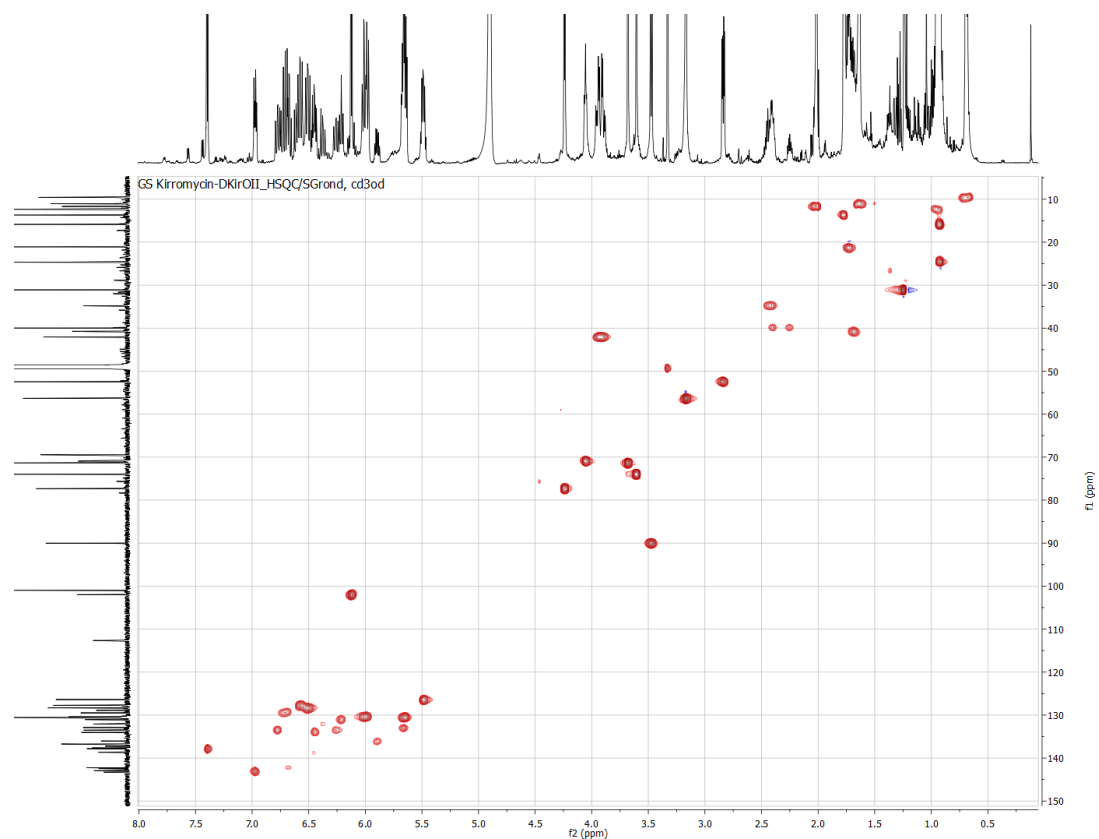


Formula S5-III Selected COSY (double dashed arrowed), TOCSY (dashed line), and HMBC (single arrowed) correlations for 30-hydroxy-5,6-dehydro-1-*N*-demethyl-16-deoxy-kirrothricin (5).

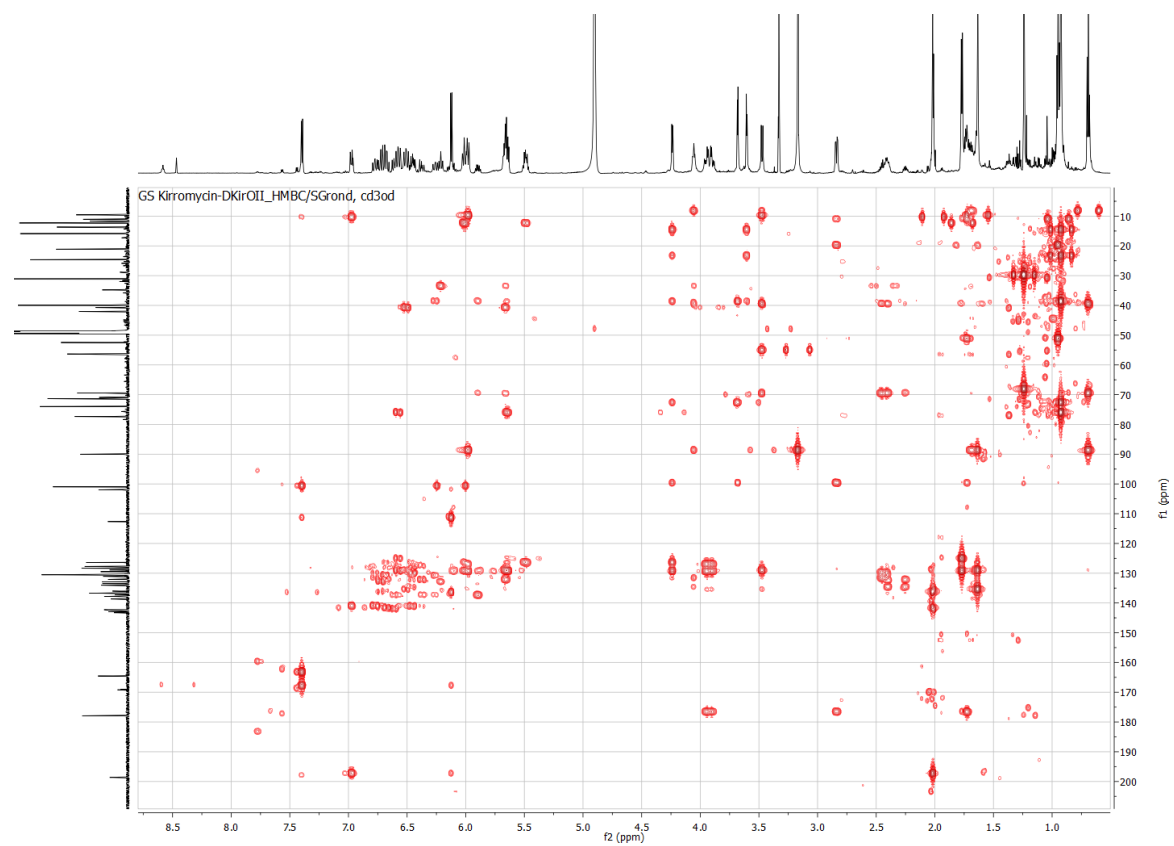
(IIIA) H-H-correlation (COSY) spectrum of 30-hydroxy-5,6-dehydro-1-N-demethyl-16-deoxy-kirrothricin (5)



(IIIB) CH-correlation (HSQC) spectrum of 30-hydroxy-5,6-dehydro-1-N-demethyl-16-deoxy-kirrothricin (5)



(IIC) Multiple bond CH-correlation (HMBC) spec. of kirromycin 30-hydroxy-5,6-dehydro-1-N-demethyl-16-deoxy-kirrothricin (5)



(IID) Key correlations highlighted for 30-hydroxy-5,6-dehydro-1-*N*-demethyl-16-deoxy-kirrothricin (5)

HMBC-NMR experiment (CD₃OD, 700 MHz) showing key correlation of the new 16-CH₂-group ($\delta_{\text{H}} = 2.40, 2.43$ ppm) with C-13, C-16, C-17 within the kirrothricin-type carbon chain of 30-hydroxy-5,6-dehydro-1-*N*-demethyl-16-deoxy-kirrothricin (5).

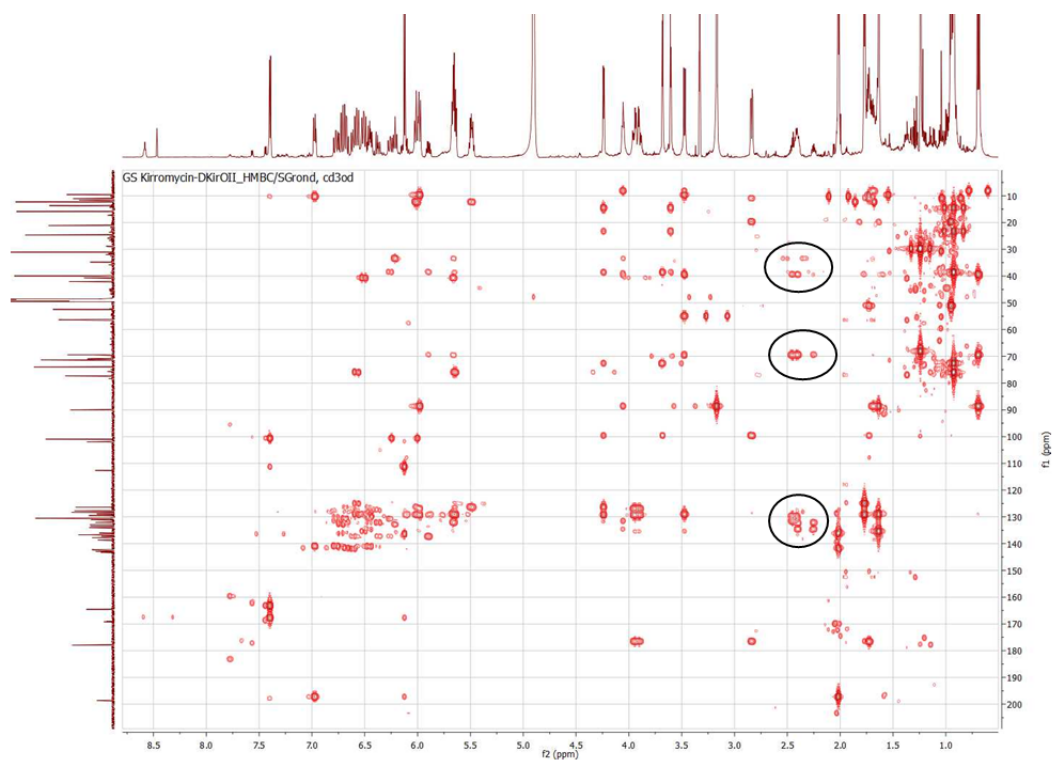
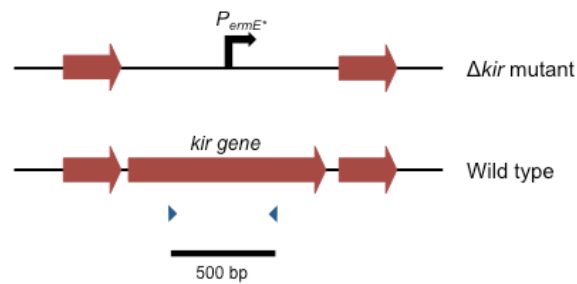


Figure S6-I – S6-II: Verification of Δkir mutants by control PCRs

Control PCRs on genomic DNA (gDNA) of $\Delta kirM$, $\Delta kirHVI$, $\Delta kirOI$, $\Delta kirOII$, $\Delta kirHIV$, $\Delta kirHV$, and $\Delta kirN$ were carried out to confirm successful double crossover (II). The use of primers (KP43 – KP56) targeting an internal 500 bp region of each gene in question (I) allowed for verification of correct mutants by the absence of bands (gene replaced by *ermE** promoter or thiostrepton resistance cassette). *Streptomyces collinus* Tü 365 (positive) (1) and water (negative) (2) controls were included for each primer pair. GeneRuler™ 1 kb DNA ladder (Fisher Scientific) (L) was used as marker.

(I)



(II)

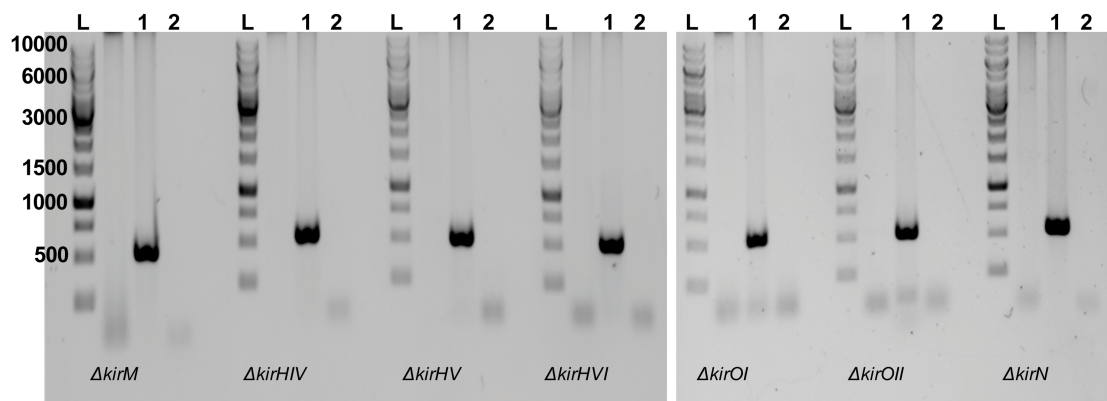
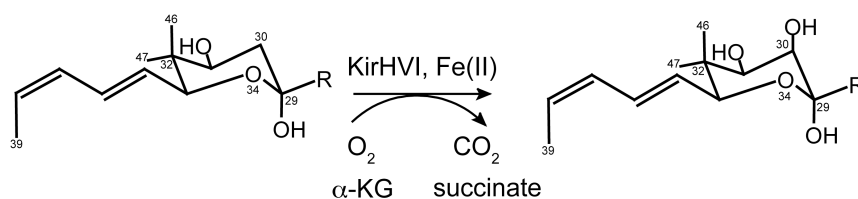


Figure S7-I – S7-III: Putative enzymatic reactions catalysed by tailoring enzymes KirHVI, KirOI, and KirOII

Genetic inactivation studies and NMR analysis enabled the prediction of the putative enzymatic reactions catalysed by the phytanoyl-CoA dioxygenase KirHVI (encoded by *kirHVI*) (**I**) and the two P450-dependent hydroxylases KirOI and KirOII (encoded by *kirOI* (**II**) and *kirOII* (**III**)).

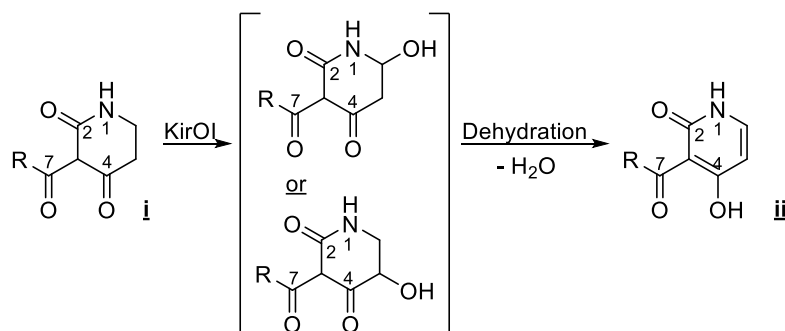
(I)

Based on its similarity to the hydroxylase Fum3p involved in fumonisin B biosynthesis¹⁰, KirHVI is postulated to induce α -ketoglutarate (α -KG)/Fe(II)-dependent hydroxylation at the C-30 position in the sugar-like moiety in kirromycin.



(II)

The cytochrome P450-dependent hydroxylase KirOI catalyses hydroxylation of either C-5 or C-6 in the δ -lactam ring of the kirromycin biosynthetic intermediate (**i**). The hydroxylated product from the Δ *kirOI* mutant was not detected in either the culture broth or the solvent extract. The intermediate can then undergo dehydration, which might be facilitated by a yet uncharacterised enzyme or an *trans*-acting dehydrogenase (DH), to form the double bond between C-5 and C-6 (**ii**). The product **ii** bears the stable pyridone ring with tautomeric equilibrium and aromatic character, presumably responsible for the stability of this dehydrated product.

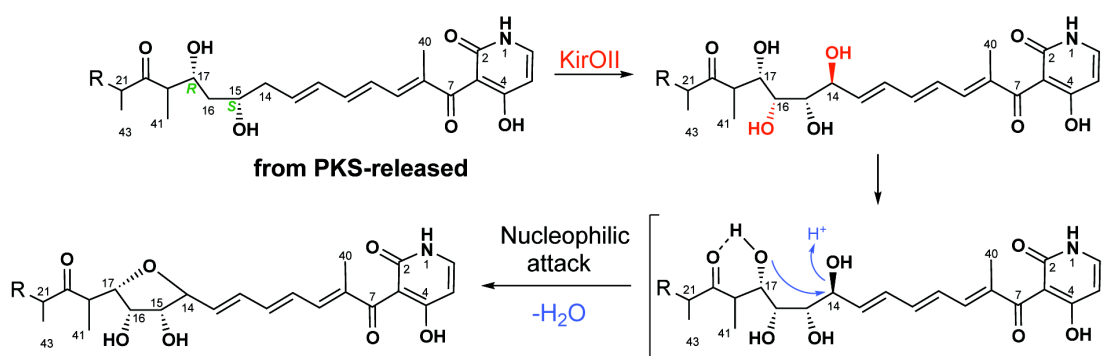


(III)

Our data suggests KirOII to be involved in formation of the tetrahydrofuran (THF) ring in the centre of the kirromycin molecule.

In case of kirromycin biosynthesis, the PKS-derived precursor molecule of kirromycin could undergo dual CH₂-hydroxylation at C-14 and C-16, possibly catalysed by the cytochrome P450 monooxygenase KirOII. The hypothesis is strengthened from the sequence comparison of KirOII to AurH (31 % identity and 49 % similarity). The cytochrome P450 monooxygenase AurH has been found to be involved in formation of the THF ring in the antifungal compound aureothin produced by *Streptomyces thioluteus*^{11,12} through the introduction of two C-O bonds. In a similar fashion, KirOII might catalyse the following step, including a classical ring-closing dehydration reaction under formation of the THF ring moiety in kirromycin. This conversion is favoured in kirromycin because of increased nucleophilicity of the C-17-hydroxyl group as a result of the hydrogen bonding in a cyclic 6-membered ring including the C-20 carbonyl group. From the Δ *kirOII* mutant, the tetraene product, named 30-hydroxy-5,6-dehydro-1-*N*-demethyl-16-deoxy-kirrothricin (**5**), is isolated from the culture broth due to chemically favoured dehydration to the stable extended conjugated double bond system between C-6 and C-15.

While this is a plausible enzymatic reaction, the scheme currently lacks an additional enzyme responsible for catalysing the reduction of C=O to C-OH at the C-20 position in kirromycin. Such an enzyme remains to be identified and characterized.



Supplementary references

1. MacNeil, D. J. *et al.* Analysis of *Streptomyces avermitilis* genes required for avermectin biosynthesis utilizing a novel integration vector. *Gene* **111**, 61–68 (1992).
2. Wolf, H. & Zähner, H. Stoffwechselprodukte von Mikroorganismen. *Arch. Mikrobiol.* **83**, 147–154 (1972).
3. Weber, T. *et al.* Molecular Analysis of the Kirromycin Biosynthetic Gene Cluster Revealed β -Alanine as Precursor of the Pyridone Moiety. *Chem. Biol.* **15**, 175–188 (2008).
4. Myronovskyi, M., Welle, E., Fedorenko, V. & Luzhetskyy, A. Beta-glucuronidase as a sensitive and versatile reporter in actinomycetes. *Appl. Environ. Microbiol.* **77**, 5370–5383 (2011).
5. Menges, R., Muth, G., Wohlleben, W. & Stegmann, E. The ABC transporter Tba of *Amycolatopsis balhimycina* is required for efficient export of the glycopeptide antibiotic balhimycin. *Appl. Microbiol. Biotechnol.* **77**, 125–134 (2007).
6. Muth, G., Wohlleben, W. & Puhler, A. The minimal replicon of the *Streptomyces ghanaensis* plasmid pSG5 identified by subcloning and Tn5 mutagenesis. *Mol. Gen. Genet.* **211**, 424–429 (1988).
7. Tong, Y., Charusanti, P., Zhang, L., Weber, T. & Lee, S. Y. CRISPR-Cas9 Based Engineering of Actinomycetal Genomes. *ACS Synth. Biol.* **4**, 1020–1029 (2015).
8. Tong, Y., Robertsen, H. L., Blin, K., Weber, T. & Lee, S. Y. in *Methods in Molecular Biology* **1671**, 163–184 (2018).
9. Frost, B. M., Valiant, M. E. & Dulaney, E. L. Antibacterial Activity of Heneicomycin. *J. Antibiot.* **32**, 626–629 (1979).
10. Ding, Y., Bojja, R. S. & Du, L. Fum3p, a 2-Ketoglutarate-Dependent Dioxygenase Required for C-5 Hydroxylation of Fumonisin in *Fusarium verticillioides*. *Appl. Environ. Microbiol.* **70**, 1931–1934 (2004).
11. He, J. & Hertweck, C. Iteration as Programmed Event during Polyketide Assembly; Molecular Analysis of the Aureothin Biosynthesis Gene Cluster. *Chem. Biol.* **10**, 1225–1232 (2003).
12. Richter, M. E. A., Traitcheva, N., Knüpfer, U. & Hertweck, C. Sequential Asymmetric Polyketide Heterocyclization Catalyzed by a Single Cytochrome P450 Monooxygenase (AurH). *Angew. Chemie* **120**, 9004–9007 (2008).